

RESEARCH ARTICLE

Sub-seasonal to seasonal prediction of rainfall extremes in Australia

Andrew D. King¹  | Debra Hudson²  | Eun-Pa Lim² | Andrew G. Marshall³ | Harry H. Hendon² | Todd P. Lane¹  | Oscar Alves²

¹School of Earth Sciences and ARC Centre of Excellence for Climate Extremes, University of Melbourne, Melbourne, Victoria Australia

²Bureau of Meteorology, Melbourne, Victoria Australia

³Bureau of Meteorology, Hobart, Tasmania Australia

Correspondence

A. D. King, School of Earth Sciences and ARC Centre of Excellence for Climate Extremes, University of Melbourne, Melbourne, Victoria, Australia.
Email: andrew.king@unimelb.edu.au

Funding information

Australian Research Council,
Grant/Award Numbers: CE170100023,
DE180100638

Abstract

Seasonal climate prediction to date has largely focussed on probabilistic forecasts for above- and below-average conditions in climate means. Here, we examine the possibility of making sub-seasonal to seasonal outlooks for daily-scale precipitation extremes in Australia. We first use observational data to show that significant relationships exist between climate modes, such as the El Niño–Southern Oscillation, and indices representing rainfall extremes across much of Australia. The strong observed teleconnections between climate modes and daily rainfall extremes suggest the potential for predictability on seasonal scales. The current Australian Bureau of Meteorology seasonal prediction system (ACCESS-S1) is examined for performance in predicting rainfall extreme indices using a range of measures. Ensemble hindcasts, consisting of 11 members initialised every month during 1990–2012, perform well for some extreme rainfall indices on short lead-times (up to 1 month). We note that at short lead-times, forecasts are aided by skilful weather prediction, so forecast performance drops at lead-times of a week or more. Forecast performance is lower in austral summer than other seasons and greater in the north and interior of the continent, particularly in the dry season, than elsewhere. The ACCESS-S1 ensemble is overconfident but exhibits some reliability in probabilistic forecasts of above- or below-average number of wet days and intensity of the highest daily maximum precipitation, especially in northern Australia. ACCESS-S1 captures the broad pattern of relationships between climate modes and rainfall extremes that are observed. For two case-studies of unusually extreme precipitation, ACCESS-S exhibits contrasting performance for forecasts of extreme rainfall anomalies beyond the first month. These results suggest that ACCESS-S1 may be used to produce outlooks for some rainfall indices, such as the number of wet days and the intensity of the wettest day, for the month ahead.

KEY WORDS

ACCESS-S, Australia, ENSO, IOD, rainfall extremes, seasonal prediction

1 | INTRODUCTION

Australia has a highly variable climate especially for rainfall (Nicholls *et al.*, 1997) with droughts and extreme rainfall events that have large economic, social and environmental impacts. The highly variable climate of Australia is, in large part, due to its position between the Indian and Pacific Oceans with much of the variability in rainfall linked to the Indian Ocean Dipole (IOD) and El Niño–Southern Oscillation (ENSO) in addition to other climate modes, such as the Southern Annular Mode (SAM) and the Madden–Julian Oscillation (MJO) (e.g. Risbey *et al.*, 2009).

It is not only mean rainfall that has strong relationships with these climate modes but also rainfall extremes (Min *et al.*, 2013; King *et al.*, 2014). For example, there are significant correlations between the Niño-3.4 index and seasonal maximum 1-day precipitation (Rx1day) totals in austral winter and spring across much of northern and eastern Australia (Min *et al.*, 2013). Similarly strong relationships between the Dipole Mode Index (DMI), representing the IOD, and Rx1day in southern Australia in austral winter and spring, and between the SAM index and Rx1day in the southeast of Australia in austral spring and summer were observed (Min *et al.*, 2013). While patterns of extreme rainfall indices are more spatially inhomogeneous than for mean rainfall, for Rx1day and the maximum consecutive 5-day rainfall totals (Rx5day) there are significant relationships with ENSO and the IOD (King *et al.*, 2014).

The strong teleconnections between slowly-evolving climate modes and Australian climate variability lend themselves to seasonal predictability. Australia has a long history of seasonal prediction (Quayle, 1929; Nicholls and Woodcock, 1981; Nicholls, 1985). It was recognised long ago that given a particular state of a climate mode is in place, for example La Niña, the slow evolution of the climate mode would mean that an increased likelihood of climate anomalies in one direction would often persist for several months. As a result, the Australian Bureau of Meteorology (BoM) made empirical seasonal predictions from 1989 based on observed teleconnections between ENSO and Australian climate variability (Nicholls, 1979; 1983; McBride and Nicholls, 1983) and subsequently the Indian Ocean teleconnection (Stone *et al.*, 1996; Drosdowsky and Chambers, 2000). The BoM developed and operationalised dynamical prediction models in the early twenty-first century (Alves *et al.*, 2003; Cottrill *et al.*, 2013) and the current operational system, the Australian Community Climate and Earth-System Seasonal model (ACCESS-S1: Hudson *et al.*, 2017), is now used to make probabilistic seasonal outlooks for sea-surface temperatures (SSTs), ENSO, the IOD and also Australian climate (including monthly- and

seasonal-average precipitation and maximum and minimum temperatures).

Given that the strong teleconnections between climate modes and Australian rainfall variability have been shown to extend to rainfall extremes, the possibility of seasonal prediction of rainfall extremes should be considered. Large-scale or persistent rainfall extremes have substantial impacts as they often result in catastrophic flooding. This was the case during the austral summer of 2010/2011 when heavy rainfall led to severe floods across much of Queensland resulting in multiple fatalities and large economic losses of several billion dollars (Australian Business Roundtable for Disaster Resilience and Safer Communities, 2016). Accurate seasonal prediction of not only the mean precipitation for the month or season, but for precipitation extremes as well, has the potential to have large economic benefits to the agricultural sector and other industries (The Centre for International Economics, 2014a; 2014b).

In this study we revisit the observed teleconnections between climate modes and different indices for rainfall extremes. Based on the observational analysis we select suitable indices where seasonal prediction may be possible and we subsequently investigate model performance in prediction of these indices in the ACCESS-S1 hindcasts. We use a range of verification statistics to assess forecast performance in ACCESS-S1 at a range of lead-times and we examine the model representation of relationships between climate modes and rainfall indices.

The remainder of the article is organised as follows: in Section 2 we discuss the datasets used and the methods applied in our analysis, in Section 3 we motivate our ACCESS-S1 analysis using observed relationships between climate modes and rainfall extremes, in Section 4 we examine the performance of ACCESS-S1 using a range of verification metrics, in Section 5 we analyse ACCESS-S1 relationships between climate modes and rainfall extremes, in Section 6 we focus on two case-studies, and in Section 7 we discuss and conclude our analysis.

2 | DATA AND METHODS

2.1 | Observational datasets

For verification of the forecasts, a gridded rainfall product was deemed most suitable for comparison. Daily rainfall data from the Australian Water Availability Project (AWAP: Jones *et al.*, 2009) for 1900–2017 were extracted on a regular 0.05° grid. The AWAP rainfall product is derived from interpolating all available *in situ* rainfall observations onto a grid using a splining technique (more details can be found in Jones *et al.* (2009)). Although there are

TABLE 1 Mean and extreme rainfall indices considered in this analysis

Index name	Description	Units	Type of index
<i>PRCPTOT</i>	<i>Total rainfall</i>	mm	Mean
<i>Rx1day</i>	<i>Maximum 1-day rainfall</i>	mm	Intensity
<i>R90PTOT</i>	<i>Rainfall on days above climatological 90th percentile</i>	mm	Intensity
<i>WD</i>	<i>Number of wet days (>1 mm)</i>	Number of days	Frequency
<i>R90P</i>	<i>Number of days above climatological 90th percentile</i>	Number of days	Frequency
<i>R10mm</i>	<i>Number of days above 10 mm</i>	Number of days	Frequency
<i>Rx1C</i>	Contribution of wettest day to total rainfall	%	Contribution

Note: These indices were examined in the observational-based analysis and the indices listed in italics were investigated further using ACCESS-S.

issues with AWAP underestimation of rainfall extremes, in regions where station data that AWAP is derived from are dense the variability in mean and extreme rainfall is captured well (King *et al.*, 2013b). In regions where stations are sparse, the AWAP product performs less well, thus a mask was applied over central Australia (selected as the region with no data coverage prior to 1930) and the region is not analysed further. The AWAP data were interpolated onto a regular 0.25° grid for all subsequent analysis.

A selection of mean and extreme rainfall indices was investigated for their relationships with climate modes (Table 1). The six extreme rainfall indices (in addition to total rainfall: PRCPTOT, sometimes also referred to as mean rainfall here) are adapted from those recommended by the Expert Team on Climate Change Detection and Indices (ETCCDI: Zhang *et al.*, 2011) and are chosen to represent different characteristics of extreme rainfall (Haylock and Nicholls, 2000) for which relationships with climate modes and seasonal predictive skill may be assessed. There are intensity-based indices, including Rx1day, frequency-based metrics, including the number of wet days (WD), and a contribution-based index, the proportion of monthly rainfall due to the wettest day (Rx1C). These indices were calculated using the AWAP dataset for 1900–2017 in each calendar month to allow the relationships between climate modes and rainfall indices to be robustly established. Two indices (R90P and R90PTot) use a climatological 90th percentile which is derived for each calendar month separately and excludes non-rain days in its calculation (otherwise in many cases the 90th percentile would be zero). Note, while the WD index is classified as an ETCCDI extreme rainfall index it is relevant to the whole statistical distribution of rainfall, not just the tail. While the WD index is not a truly extreme index it does represent a useful alternative characteristic of rainfall to PRCPTOT.

To examine observed extreme rainfall relationships with coupled ocean–atmosphere climate modes, a dataset of observed SSTs was used. The Met Office Hadley Centre Sea Ice and Sea Surface Temperature product was analysed

(HadISST: Rayner *et al.*, 2003). The monthly SST data were used to compute the Niño-3.4 index to represent ENSO (170°W–120°W, 5°S–5°N), the Dipole Mode Index to represent the IOD (Western pole: 50°E–70°E, 10°S–10°N, Eastern pole: 90°E–110°E, 10°S–0°N) (Saji *et al.*, 1999), and the north Australian SST index (110°E–150°E, 15°S–0°N) (Nicholls, 1984; Catto *et al.*, 2012). Area-average SSTs were computed for the relevant regions and the climate mode indices were computed by detrending the data in each calendar month individually by subtracting a 31-year moving average. In the case of the DMI, the detrending was performed before the difference between the western and eastern poles was computed, but the sensitivity to this choice is minimal.

The relationships between climate modes and different extreme rainfall indices were assessed through computing Spearman rank correlation coefficients, to account for non-normal distributions of extreme indices across most of Australia in most months. The areas of Australia (excluding the masked region of central Australia) where these correlations are significant at the 5% level were aggregated for summarising the relationships between the climate modes and each rainfall index.

2.2 | The ACCESS-S1 hindcasts

ACCESS-S1 is a state-of-the-art seasonal prediction model system used operationally by the BoM (Hudson *et al.*, 2017). The current version of the model is the same as the UK Met Office model GloSea5-GC2 (MacLachlan *et al.*, 2015) but the ensemble generation scheme, ensemble size and the configuration of the system for operational forecasting differ (see Hudson *et al.* (2017) for further details). The ACCESS-S1 hindcasts have been used previously to evaluate the model for its skill in temperature and precipitation totals over Australia (Hudson *et al.*, 2017), the evolution of ENSO, the IOD and MJO (Hudson *et al.*, 2017; Marshall and Hendon, 2019), skill for

SST (de Burgh-Day *et al.*, 2019; Smith and Spillman, 2019), and tropical cyclone frequency and location (Camp *et al.*, 2018). Here we analyse ACCESS-S1 performance in prediction of extreme precipitation indices.

The hindcasts used in this analysis cover the 1990–2012 period with 11-member ensembles initialised four times per month each running for 7 months. For this analysis, we primarily used the hindcasts initialised on the first of each month and calculated each rainfall index for each calendar month and ensemble member at lead-0, lead-1 month, and lead-2 months (e.g. for forecast verification in March 1990, leads-0, 1 and 2 correspond to runs starting 1 March 1990, 1 February 1990 and 1 January 1990, respectively).

We used the ACCESS-S1 hindcasts that have been calibrated to AWAP daily rainfall using a quantile-matching method applied to daily precipitation in 11-day windows (Bureau of Meteorology, 2019). The calibrated data are on the same regular 0.05° grid as AWAP and for this study were interpolated to the same regular 0.25° grid as was applied to AWAP. The high-resolution 0.05° data are not required for the verification of seasonal forecasts across the entire continent, so re-gridding was performed to a coarser resolution to reduce computational costs. The resolution dependence of the results was tested using a coarser grid, at a lower resolution than the raw model output, and it was found to not have a large effect (not shown). Despite the calibration of ACCESS-S1 hindcasts to AWAP, there are still differences between ACCESS-S1 hindcasts and AWAP over the common 1990–2012 period in the average values of each extreme rainfall index (see Figure S1 for an example based on Rx1day). As a result, the ACCESS-S1 anomalies were calculated relative to ACCESS-S1 rather than AWAP as discussed further in Section 2.3.

2.3 | Anomaly calculation and forecast verification statistics

The rainfall indices were evaluated in ACCESS-S1 relative to AWAP in anomaly space. In AWAP the anomalies for each rainfall index in each calendar month were calculated relative to all other years in the same calendar month at the same location. For example, Rx1day in January 2000 was calculated as an anomaly from the median of all other January Rx1day values in the 1990–2012 period excluding January 2000 itself (i.e. cross-validation). The median was used, as in many cases the statistical distributions of extreme rainfall indices are strongly positively skewed.

As the ACCESS-S1 model has biases compared to AWAP, the model itself was used to construct climatologies. The same principle of computing the index anomaly from all equivalent values was applied (same location, calendar month, and for ACCESS-S1, the same lead time

also). The climatology is also composed of all 11 ensemble members. For example, Rx1day in January 2000 at lead-0 in ACCESS-S1 ensemble member five was calculated as an anomaly relative to the median of all other January Rx1day values in ACCESS-S1 at lead-0 for 1990–2012 using all ensemble members but excluding January 2000 itself. All subsequent analysis of ACCESS-S1 was performed in anomaly space. Also, while performance analysis of ACCESS-S1 could be undertaken for different points in the distribution (e.g. upper or lower terciles or deciles), we focus much of our analysis on performance in forecasting above-median conditions. This is in part because this is the primary mode of delivery for the BoM seasonal outlooks and also because the verification statistics tend to be more robust where sample sizes are larger (e.g. Wilks, 2010).

There is a plethora of metrics that may be used to undertake seasonal prediction verification with different measures designed to represent different aspects of forecast performance (e.g. Wilks, 2011; Vitart *et al.*, 2019). A selection of metrics designed to examine different aspects of the performance of the ACCESS-S1 hindcast ensemble in predicting rainfall extremes were used here. Most of these metrics are displayed using maps or aggregated data across Australia with adaptations to these metrics designed to account for non-Gaussian distributions of the extreme indices and greater ease in the visualisation and interpretation of results.

Firstly, mapped Spearman rank correlation coefficients were computed between ensemble median ACCESS-S1 values and AWAP values for each calendar month and each index at lead-0 and lead-1. The correlation coefficients allow for the temporal variations of the indices between the observational product and the model to be compared. To condense this information for easier comparison between indices, the Australia- and state-average correlation coefficients were calculated for all indices and calendar months. These are Pearson correlations as the Fisher Z-transform was used to calculate area-average values and compute associated correlation coefficients. Matrices of these Australia- and state-average correlation coefficients allow for visual comparison of this measure of model performance between states, indices and calendar months. The Australia-average correlation statistics were also calculated using the other initialisation dates within each month (9th, 17th and 25th) to examine the performance of ACCESS-S1 at more lead-times. These were also calculated for all indices and calendar months using the Fisher Z-transform technique.

The proportion correct (PC) was also employed as a metric to assess the fraction of instances where ACCESS-S1 was correct in a seasonal prediction. This was applied to each index by examining the proportion

TABLE 2 Months used in composites of forecasts during ENSO, IOD and north Australian SST mode phases

Climate mode	Calendar months analysed	Years extracted in positive phase	Years extracted in negative phase
ENSO (Niño-3.4)	October	1991, 1994, 1997, 2002, 2009	1998, 1999, 2007, 2010, 2011
IOD (DMI)	September	1994, 1997, 2002, 2006, 2012	1992, 1996, 1998, 2005, 2010
N. Australian SSTs	July	1990, 1996, 1998, 2009, 2010	1991, 1993, 1994, 1997, 2000
SAM (Marshall index)	November	1992, 1998, 1999, 2001, 2010	1994, 1996, 1997, 2000, 2011

of instances where the ACCESS-S1 ensemble median anomaly was of the same sign as the AWAP anomaly.

The Brier Skill Score (BSS) was calculated to examine how skilful the ACCESS-S1 hindcast simulations are relative to climatology. This was also applied to all indices and all locations across Australia in each calendar month using probabilistic forecasts calculated using the ACCESS-S1 ensemble and comparing to AWAP. The BSS was computed for forecasts of the probability of above-average values of each index.

Rank histograms show if an ensemble of forecasts appropriately samples forecast uncertainty by comparing observations with the range of the ensemble member forecasts (Wilks, 2011). Goodness of ensemble forecasts is indicated by even distribution of the frequency of observations in all ranks of ensemble forecasts. Rank histograms were used to examine whether ACCESS-S1 is over- or under-confident in the ensemble spread for different indices and locations. The most frequent rank of AWAP relative to the ACCESS-S1 ensembles was plotted to produce maps and warm season months (defined as November to April) and cool season months (May–October) were aggregated to increase sample size for compiling the rank histograms. In addition to these maps, box-plots displaying the frequency of observation in each rank for all locations across Australia were constructed. An estimate of the 95% confidence interval on the frequency of ranks that could be expected by chance was made. This was computed by 138 random draws from a uniform distribution of 12 values. The 138 draws from this distribution matches the number used in forming the rank histograms which are each based on six values (for the 6 months in the warm and cool seasons) over a 23-year hindcast. This process was repeated 10,000 times and for a random rank the 2.5th and 97.5th percentiles of frequency were estimated. Values outside of this range are deemed to be unlikely to occur due to chance.

The reliability of the ACCESS-S1 probabilistic forecasts was computed by binning the forecast probabilities into 11 categories spanning from a probability of 0 to 100%, and computing the corresponding observed probability of the event for those forecasts. Reliability is plotted on a reliability diagram, but here we also use maps to

represent reliability in indices at individual locations across Australia. As for the rank histograms, reliability was computed on composites of warm season and cool season months rather than individual calendar months to generate a larger sample size.

2.4 | Further ACCESS-S1 evaluation

In addition to the metrics described above, the relationship between climate modes and rainfall indices in ACCESS-S1 was compared with observed relationships. For the calendar months with the largest areal signature of statistically significant ($p < .05$) observed correlations between each climate mode and total precipitation (as listed in Table 2 and extracted from Figure 1), the observed and simulated relationships were compared. For SAM, the relationship with rainfall means and extremes is strongest in late spring and early summer (Min *et al.*, 2013; Hendon *et al.*, 2014; Lim and Hendon, 2015), so November was chosen.

The relationships between climate modes and rainfall means and extremes in ACCESS-S1 were investigated in two different ways. Firstly, using the calendar months with the strongest observed relationships between each of the four climate modes and mean rainfall, the regression coefficient of each rainfall index onto each climate mode over 1990–2012 was computed for each location across Australia using both observed climate modes and rainfall indices, and ACCESS-S1 ensemble-mean simulated climate modes (at leadtime-0 months) and rainfall indices. This allows the observed and simulated teleconnections to be compared directly.

Secondly, the 5 years where each of the calendar months that ENSO, the IOD, north Australian SSTs and the SAM were in their most positive and negative phase based on the observational data during the 1990–2012 hindcast period were composited (Table 2). The median difference (to limit sensitivity to outliers) between rainfall indices in the positive and negative phases of each index was computed for each of AWAP and ACCESS-S1. The Spearman rank pattern correlation coefficient was computed between AWAP and ACCESS-S1 to allow for a quantitative measure of model performance in the patterns of the

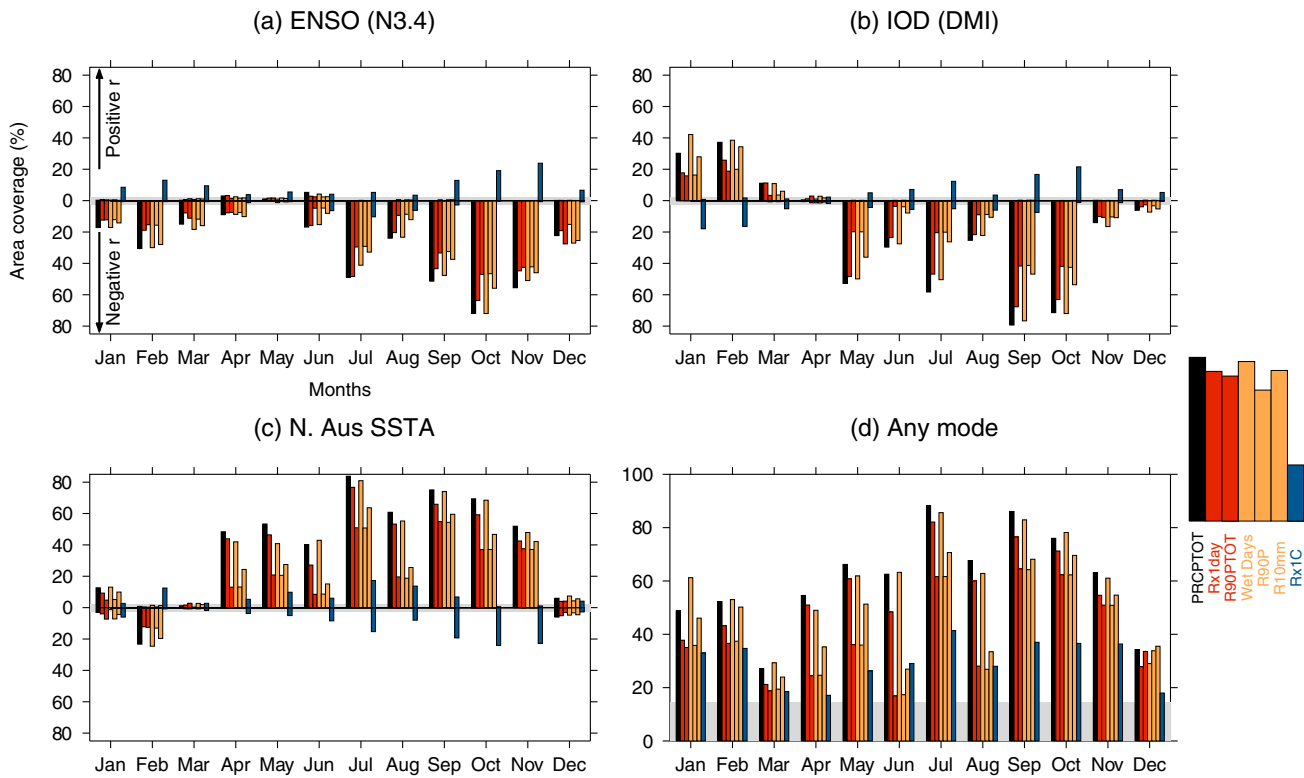


FIGURE 1 Bar graphs showing the area of Australia with significant concurrent Spearman rank correlations (p -value $< .05$) between mean and extreme rainfall indices and (a) Niño-3.4, (b) DMI, (c) north Australian SSTs, and (d) any of the three climate modes. Bars in (a–c) are plotted either above or below the zero line for positive or negative correlations respectively. The grey region indicates the area of significant correlations that might be expected by chance. The legend on the right indicates which bars correspond to which indices [Colour figure can be viewed at wileyonlinelibrary.com]

mean and extreme rainfall anomalies associated with each climate mode. This analysis allows ACCESS-S1 to be compared with observations for specific periods of strong climate mode phases. This provides a test of performance in prediction of climate mode–extreme rainfall relationships.

In addition, during the hindcast period of 1990–2012 there were several occasions when impactful large-scale extreme rainfall events occurred. The ability of ACCESS-S1 to predict anomalies of mean and extreme precipitation in the case of two such events was examined. The two events investigated in more detail were December 2010, when extreme rainfall resulted in severe flooding across large areas of Queensland (van den Honert and McAneney, 2011), and June 2007, when flooding occurred in several areas of Australia some of which was associated with an East Coast Low system affecting New South Wales (Mills *et al.*, 2010). The anomalies in ACCESS-S1 mean and extreme precipitation indices at lead-0, lead-1 month and lead-2 months were compared with the observed anomalies. Again, Spearman rank pattern correlation coefficients between AWAP and ACCESS-S1 were computed. The correlation coefficients were computed between each ACCESS-S1 ensemble member and AWAP.

3 | OBSERVED RELATIONSHIPS BETWEEN CLIMATE MODES AND EXTREME RAINFALL INDICES

The observed relationships between ENSO, IOD and north Australian SSTs, and rainfall indices were examined by correlating representative indices for these climate modes with rainfall indices (Table 1). The relationships between these climate modes and rainfall means and extremes are strongest in different areas and seasons (Risbey *et al.*, 2009; Min *et al.*, 2013; King *et al.*, 2014). To condense this information, Figure 1a–c shows bar plots of the area of Australia for which there are significant correlations ($p < .05$) between indices representing ENSO, IOD and north Australian SSTs and each rainfall index, respectively. The strongest relationships between these climate modes and rainfall indices tend to be in austral winter and spring with the area under significant correlation peaking earliest for north Australian SSTs (in around July), then peaking for the IOD in September and ENSO in October. In general, the bar plots indicate stronger relationships between the climate modes and mean rainfall than for extreme rainfall indices (Min *et al.*, 2013, King *et al.*, 2014), but there is

a large difference in results between some of the extreme rainfall indices. In particular, the contribution metric used here, Rx1C, shows much weaker relationships with all the climate modes than the other indices exhibit.

The area of Australia that exhibits a significant relationship between rainfall indices and any of ENSO, the IOD and north Australian SSTs for a given calendar month was aggregated as this gives an indication of the potential for predictability more generally (Figure 1d). Unsurprisingly, given the results shown in Figure 1a–c, austral winter and spring are the times of year when Australian mean and extreme rainfall indices exhibit more widespread significant relationships with climate modes. There are months where WD has more widespread relationships with climate modes than are observed for mean rainfall, but the Rx1C index exhibits substantially weaker relationships than the other indices. Based on this observational analysis we examine the predictive skill of these extreme rainfall indices in ACCESS-S1 (aside from Rx1C).

4 | PERFORMANCE OF EXTREME RAINFALL PREDICTION IN ACCESS-S1

Performance in ACCESS-S1 predictions was first assessed using Spearman's rank correlation coefficient based on the ensemble-median of the hindcast set and AWAP for lead-0. These are shown for each calendar month for Rx1day in Figure 2 and, for most of Australia and in most calendar months, the correlations are positive and often significant. There is a general pattern towards higher correlations in the interior of the continent and for the weaker correlations to be in late spring and early summer months. Unfortunately, the performance of ACCESS-S1 is better during drier times in the year when the Rx1day totals tend to be lower (Figure S2).

To condense the information from these correlation maps, correlation coefficient matrices were produced using all indices for Australia-average values and for each state and territory of Australia at lead-0 (Figure 3). Note, these are Pearson correlation coefficients due to the averaging applied to Z-scores to conserve normality. The distinct seasonal cycle in forecast performance, as measured by correlation coefficients, is apparent in most of the mainland states and territories, but there are different levels of performance between indices. Aside from mean precipitation, the WD index also exhibits stronger correlations than are seen for the other indices. The R90PTot index shows generally weak skill with the R90P and R10mm indices also performing relatively poorly in line with the weaker climate mode relationships found for these indices (Figure 1). The general pattern of greater

forecast performance in the north and east is also clear with ACCESS-S1 performing better, using the correlation coefficient measure, in Queensland and the Northern Territory than elsewhere.

A similar plot for lead-1 month correlations was also produced (Figure 4). These longer lead forecasts exhibit far poorer model performance than the lead-0 forecasts. Overall, in many cases, correlation coefficients are still positive but few are statistically significant. While all the correlations are relatively weak at this lead-time, they are still higher in northern Australia, albeit at a drier time of year, and for PRCPTOT and WD than for other indices.

The effect of lead-time on model performance was investigated using ACCESS-S1 simulations initialised at other times within the month as well as the 1st of the month simulations. Figure 5 shows the Australia-average correlations between ACCESS-S and AWAP for (a) Rx1day and (b) PRCPTOT in each calendar month using simulations initialised on 9th, 17th and 25th in the months prior to the month of interest. The performance of ACCESS-S decreases even at lead-times of around 1 week or half a month with a tendency for greater reduction in model performance with lead-time during the warm season months than in the cool season. The remaining analysis is based on the 1st of the month simulations only.

The proportion correct (PC) was computed comparing the sign of the ACCESS-S1 ensemble median anomaly with the sign of the observed anomaly (Rx1day at lead-0; Figure S3). The PC results largely mirror those found using the correlation coefficients with PC falling below 0.5 (i.e. negative skill compared to a climatological forecast) in some areas of Australia in late spring and early summer, but generally higher in other seasons. The PC metric performs poorly where the median value is at or near zero (i.e. no heavy rainfall has occurred), which is true for several indices considered here, especially in northern Australia in the dry season. Australia- and state-average values of PC (not shown) are less useful than the correlation coefficient equivalent values (Figure 3) due to the high frequency of zero-values and skewness in statistical distributions for many indices. For forecasts of the probability of above-average conditions, we use the Brier Skill Score (BSS) computed relative to a climatological forecast. The BSS shows skill above climatology over most of Australia in most months for PRCPTOT and some extreme indices (see Figure S4 for an example for Rx1day at lead-0). Once again, December shows substantially less skill than is found in other calendar months. Skill, as measured by the BSS, is above climatology in most of northern Australia and in most months outside late spring and early summer.

To better understand the characteristics of the ACCESS-S1 ensemble, we used rank histograms comparing the frequency of AWAP ranks relative to

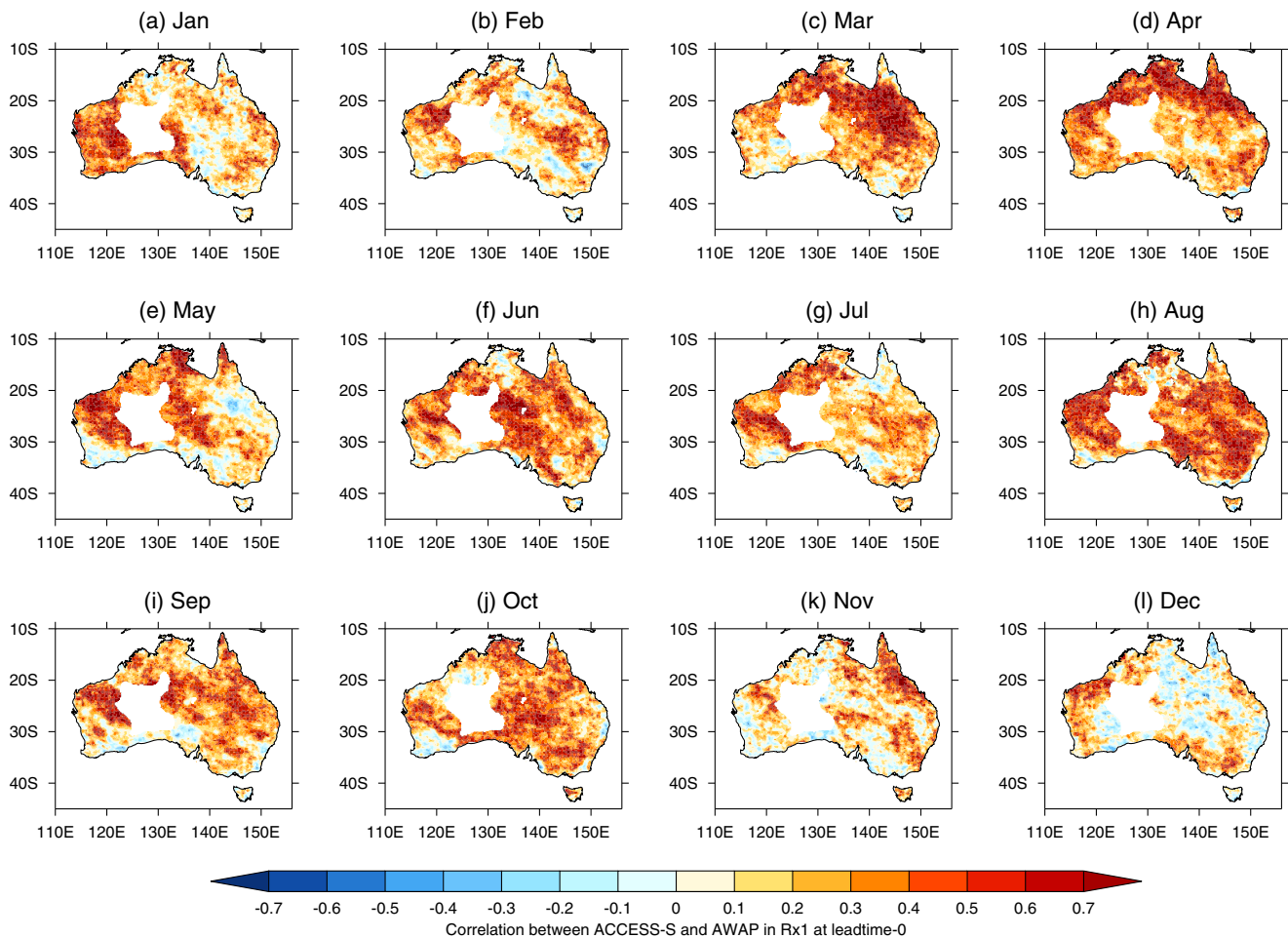


FIGURE 2 (a–l) Spearman's rank correlation coefficients in Rx1day between AWAP and the ensemble median ACCESS-S1 value at leadtime-0 for each calendar month from 1990 to 2012. Stippling indicates correlations significant at the 5% level [Colour figure can be viewed at wileyonlinelibrary.com]

different points within the ACCESS-S1 ensemble. Over most of Australia, AWAP monthly rainfall totals and Rx1day tend to be too frequently outside of the lowest rank of the ensemble, indicating that ACCESS-S1 ensemble has a wet bias (Figure S5). In contrast, AWAP WD anomalies are too frequently outside of the highest rank of the ensemble, indicating that the number of wet days is systematically underpredicted by ACCESS-S1. Aggregating across Australia we observed that for PRCPTOT and Rx1day in most places the observed anomalies are below the entire ACCESS-S1 ensemble considerably more than could be expected by chance (as evidenced by the frequency in the lowest rank outside of the grey area in Figure 6). The ACCESS-S1 ensemble is under-dispersive for PRCPTOT, Rx1day and WD in both the warm season and cool season as implied by the rank histogram tending to be U-shaped because the ensemble members tend to be too similar and biased against the verification. The ACCESS-S1 ensemble is more dispersive for WD than other indices, but this may be in part due to the discrete

values this index can take even in anomaly space when the climatological value is a median rather than a mean.

The reliability of probabilistic forecasts relates to how well the predicted probabilities of an event correspond to their observed frequencies and, like the rank histogram, can provide an indication of forecasting bias. The reliability of lead-0 Rx1day forecasts in the warm season (Figure 7) and cool season (Figure S6) is visualised first through maps of the observed frequency of above-average anomalies, given different fractions of the ACCESS-S1 ensemble are above average. The maps illustrate that as an increasing fraction of the ACCESS-S1 ensemble is above average, there is a higher observed frequency of above-average values. There is a great deal of noise between locations in this pattern such that reliability diagrams based on single locations and with relatively low sample size would not be informative. To account for this issue, the reliability was also plotted on traditional reliability diagrams, aggregating values from across Australia to produce box plots (Figure 8). These show that the forecasts for PRCPTOT,

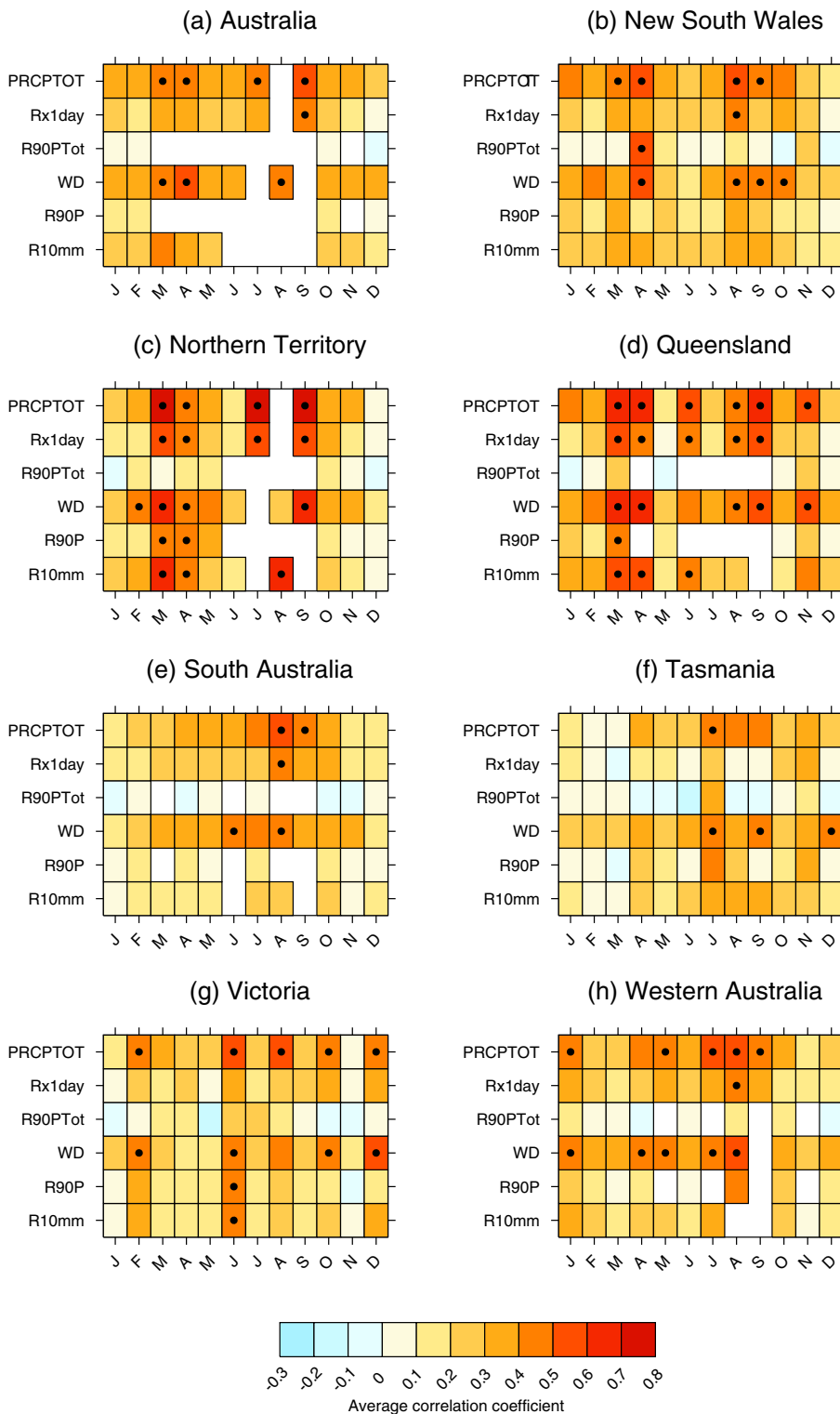
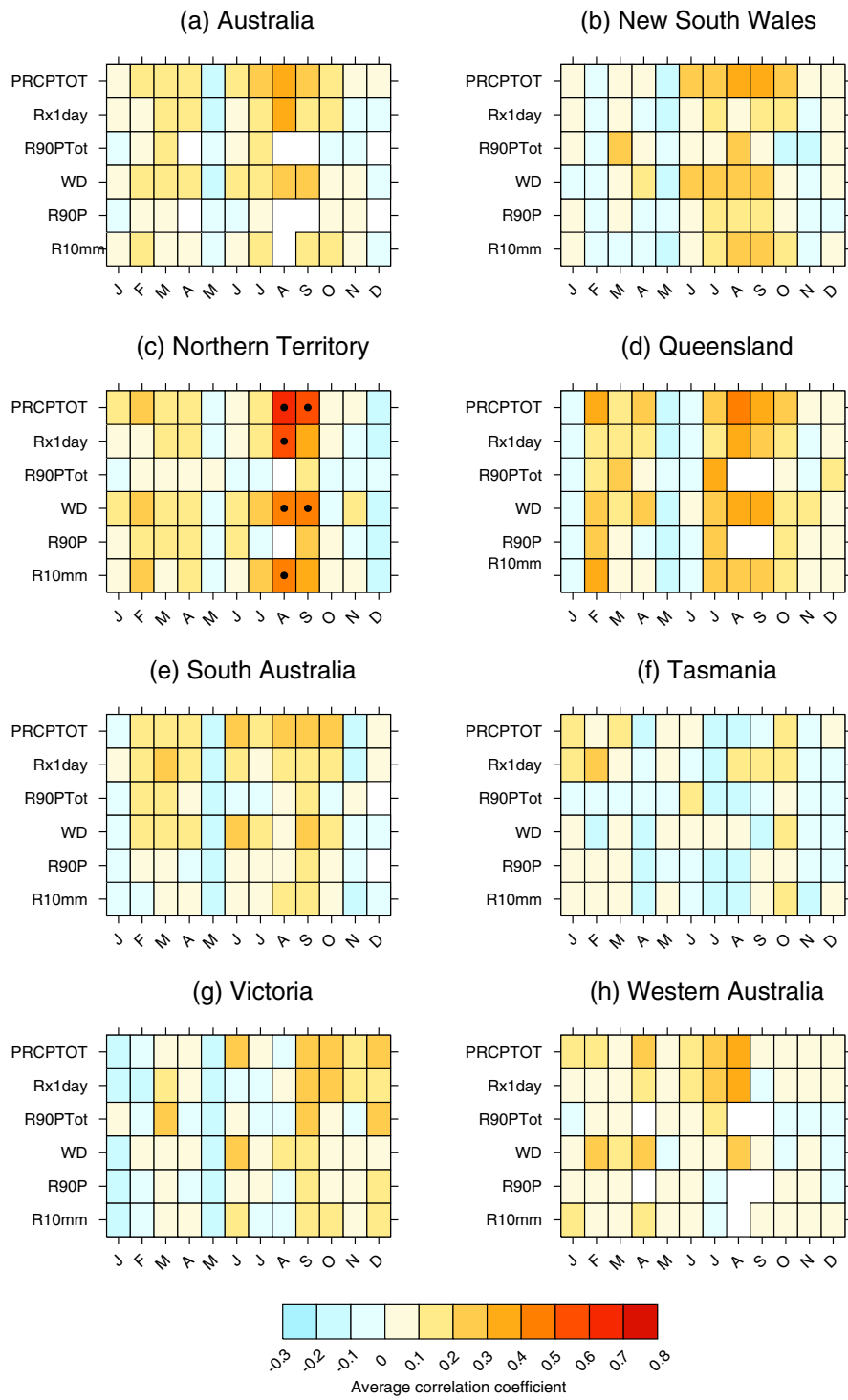


FIGURE 3 (a-h) Area-average correlation coefficient matrices for each state of Australia in each calendar month and index at leadtime-0. Black dots indicate correlations significant at the 5% level. These Pearson correlation coefficients are derived by applying the Fisher Z-transform and area-averaging on Z-scores. Grid cells in white show areas where the index has too few non-zero values for reliable correlation calculation [Colour figure can be viewed at wileyonlinelibrary.com]

Rx1day and WD are overconfident (i.e. under-dispersed), for example probabilistic forecasts of under 10% chance of above-average conditions are commonly associated with observed frequencies of above-average conditions around 20%, and, at the upper end of the scale, forecasts of above 90% chance of above-average conditions are commonly associated with observed frequencies of above-average

conditions around 80%. Despite the overconfidence in the forecasts, the majority of the distributions displayed through box plots are in the dark grey region indicating there is some skill over a climatological forecast. Overall, the reliability diagrams suggest slightly greater skill and reliability over more of Australia in the PRCPTOT and WD forecasts than the Rx1day forecasts. The reliability

FIGURE 4 (a-h) As Figure 3 but for lead-1 month correlation coefficients [Colour figure can be viewed at wileyonlinelibrary.com]



diagrams were also plotted for northern and southern Australia, defined as areas north and south of 26°S respectively (Figures S7 and S8). These point to a greater degree of overconfidence in the ACCESS-S1 ensemble aggregating across southern Australia compared with northern Australia in both the warm and cool seasons. This regional difference in ACCESS-S1 ensemble performance is also suggested by the mapped reliability plots (Figures 7 and S6).

5 | RELATIONSHIPS TO CLIMATE MODES

The slow evolution of climate modes and their strong teleconnections to Australian climate give rise to high potential predictability for the continent. As such it is vital that the relationship between climate modes, such as ENSO, and Australian rainfall indices are well represented for

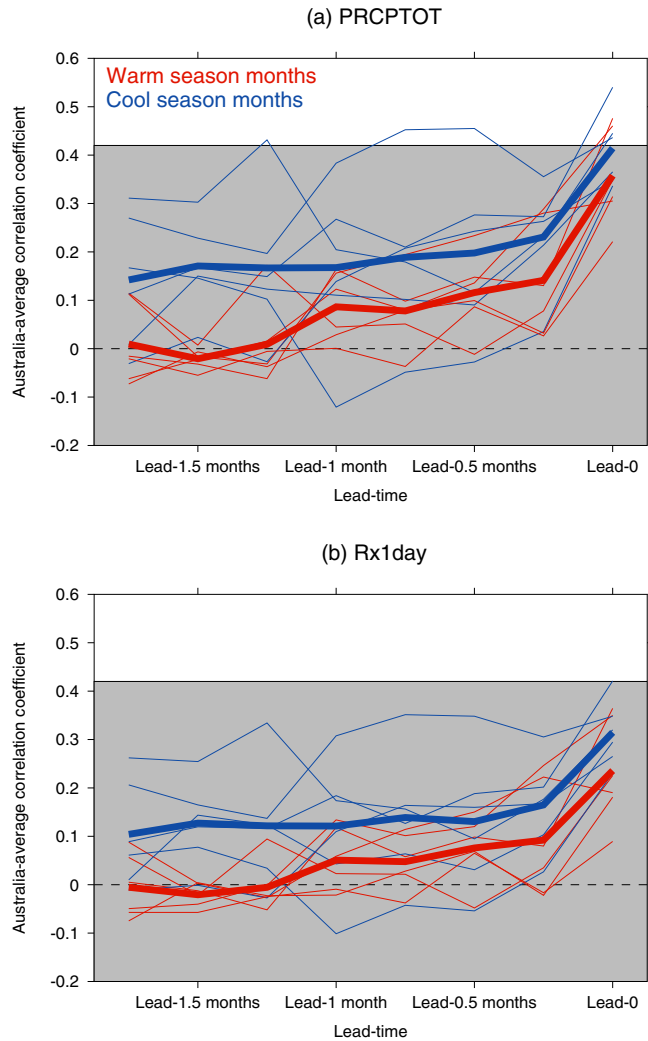


FIGURE 5 Australian-average correlation coefficients between ACCESS-S and AWAP calculated for each calendar month at every lead-time from 1.75 months in advance to lead-0 for (a) PRCPTOT and (b) Rx1day. Each thin line represents a different calendar month. These Pearson correlation coefficients are derived by applying the Fisher Z-transform and area-averaging on Z-scores. The thicker lines represent warm and cool season average correlations at each lead-time computed by averaging the Z-scores from each month at that lead-time. The grey area shows correlations non-significant at the 5% level [Colour figure can be viewed at wileyonlinelibrary.com]

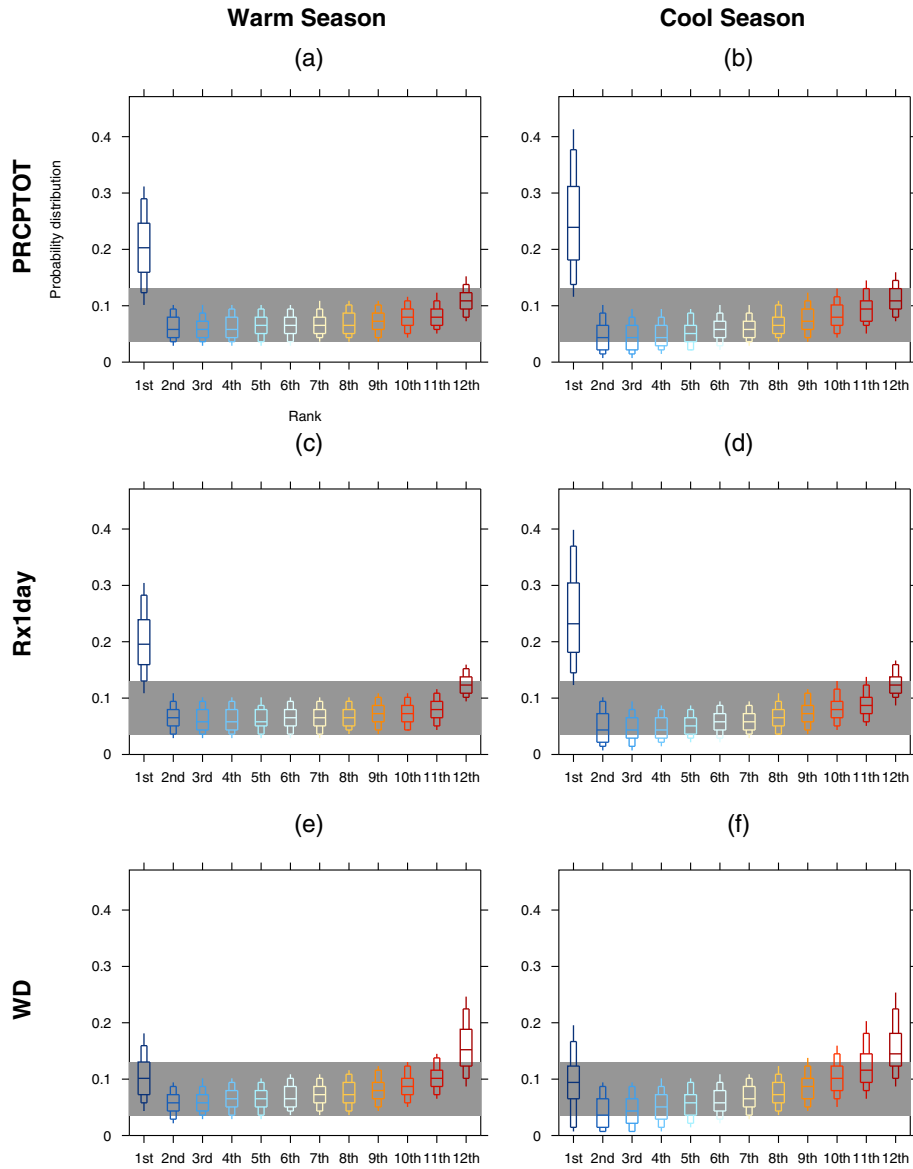
there to be confidence that ACCESS-S1 may be useful for the sub-seasonal to seasonal prediction of rainfall indices. It has been shown previously that ACCESS-S1 exhibits skill in multi-week to seasonal forecasts of ENSO, IOD and SAM (Hudson *et al.*, 2017), so accurate representation of teleconnections to Australian climate should aid skill in prediction of rainfall indices.

To investigate how Australian rainfall indices are associated with climate modes, the calendar months with the largest areal extent of significant correlations between

ENSO, the IOD and north Australian SSTs and mean rainfall were selected (Figure 1; Table 2). The observed and simulated teleconnections between these climate modes and the rainfall indices were compared by regressing each observed and simulated (model lead-0) rainfall index onto the corresponding observed and simulated climate mode indices (Figure 9). Note, the use of the ACCESS-S1 ensemble mean climate mode slightly reduces the amplitude of regression coefficients relative to the observed climate modes. The regression maps are similar between AWAP and ACCESS-S1 with the model capturing the broad relationships in the observed data across the mean and extreme rainfall indices and the different climate modes. The observed ENSO relationships with all three extreme indices shown here are stronger than in ACCESS-S1 over most of northern and eastern Australia. The observed IOD relationship with mean and extreme rain indices tends to be stronger in the south of Australia but in the model the teleconnection may be shifted slightly (this is seen most clearly in Figure 9s,t). There is more spatial inhomogeneity in the observed regression maps than in ACCESS-S1 as an ensemble-mean is used in the model.

To examine how the ACCESS-S1 model performs when the climate modes are in strongly positive or negative phases, another test was performed. The 5 years with the most extreme values of each climate mode in each direction, using the observational data only, were selected and used to produce composite median differences in the rainfall indices in both AWAP and ACCESS-S1. For example, in AWAP, La Niña Octobers are wetter on average than El Niño Octobers across most of the continent and ACCESS-S1 reproduces this pattern well (Figure 10a,b). This tendency for wetter conditions in La Niña phases also holds true for Rx1day and WD and ACCESS-S1 captures the corresponding patterns well also (Figure 10i,j,q,r). The differences in mean and extreme rainfall indices between cases of positive and negative IOD and positive and negative north Australian SST extremes are also captured in general in ACCESS-S1 (Figure 9). The SAM also exhibits a strong teleconnection to Australian rainfall (Risbey *et al.*, 2009; Min *et al.*, 2013; Lim and Hendon, 2015) so a good representation of this relationship in ACCESS-S1 is important especially in southern Australia and on the east coast. The SAM is noisier than the other climate modes and the observed differences in mean and extreme precipitation between SAM phases in November show less of a clear pattern than for ENSO, the IOD, or north Australian SSTs in their selected months. Nonetheless, ACCESS-S1 broadly captures the expected pattern of reduced mean rainfall, less intense extreme rain days, and fewer wet days in eastern Australia in negative SAM relative to positive SAM phase.

FIGURE 6 (a-f) Rank histograms showing the frequency of ranks of the observed value relative to the ACCESS-S1 ensemble in locations across Australia. The box-plots show the frequency at the median location with the large box representing the interquartile range, the narrower box representing the 10th–90th percentile range, and the whiskers showing the 5th–95th percentile locations. The grey zone represents an estimate of the 95% confidence interval of rank frequencies that could be expected by random chance for the same sample size as is available here [Colour figure can be viewed at wileyonlinelibrary.com]



6 | CASE-STUDY ANALYSES: DECEMBER 2010 AND JUNE 2007

It is of particular importance that ahead of periods of extreme weather, seasonal predictions are accurate enough to allow for planning well ahead of time to mitigate the risks associated with these events. One warm season and one cool season case-study of particularly extreme rainfall events were investigated in more detail. Firstly, the month of December 2010 which saw record-breaking rains and extreme flooding in Queensland especially (van den Honert and McAneney, 2011) was selected. This event occurred during a strong La Niña, which is typically associated with very wet conditions in the northeast of Australia (Risbey *et al.*, 2009; Klingaman *et al.*, 2013), and very high local SSTs also increased the precipitation totals during this event (Evans and Boyer-Souchet, 2012). The

observed PRCPTOT, Rx1day, and WD anomalies illustrate the wetter-than-average conditions across all these indices during December 2010 (Figure 11d,h,l). At lead-0 (i.e. 1 December 2010 simulations), the ACCESS-S1 ensemble median anomalies show a very similar pattern to the observed anomalies. The pattern correlations at this lead-time with the observed anomalies are high, except in Rx1day, but this is principally due to the higher spatial inhomogeneity in that index. At longer lead-times of lead-1 month (1 November 2010) and, to a lesser extent, lead-2 months (1 October 2010) there is still an indication of wetter conditions likely in December 2010, but the signal is less clear and the pattern of very wet conditions observed in southeast Queensland and eastern New South Wales is not forecast. As seasonal forecasts are usually communicated in probabilistic terms, it is promising that a majority of ensemble members

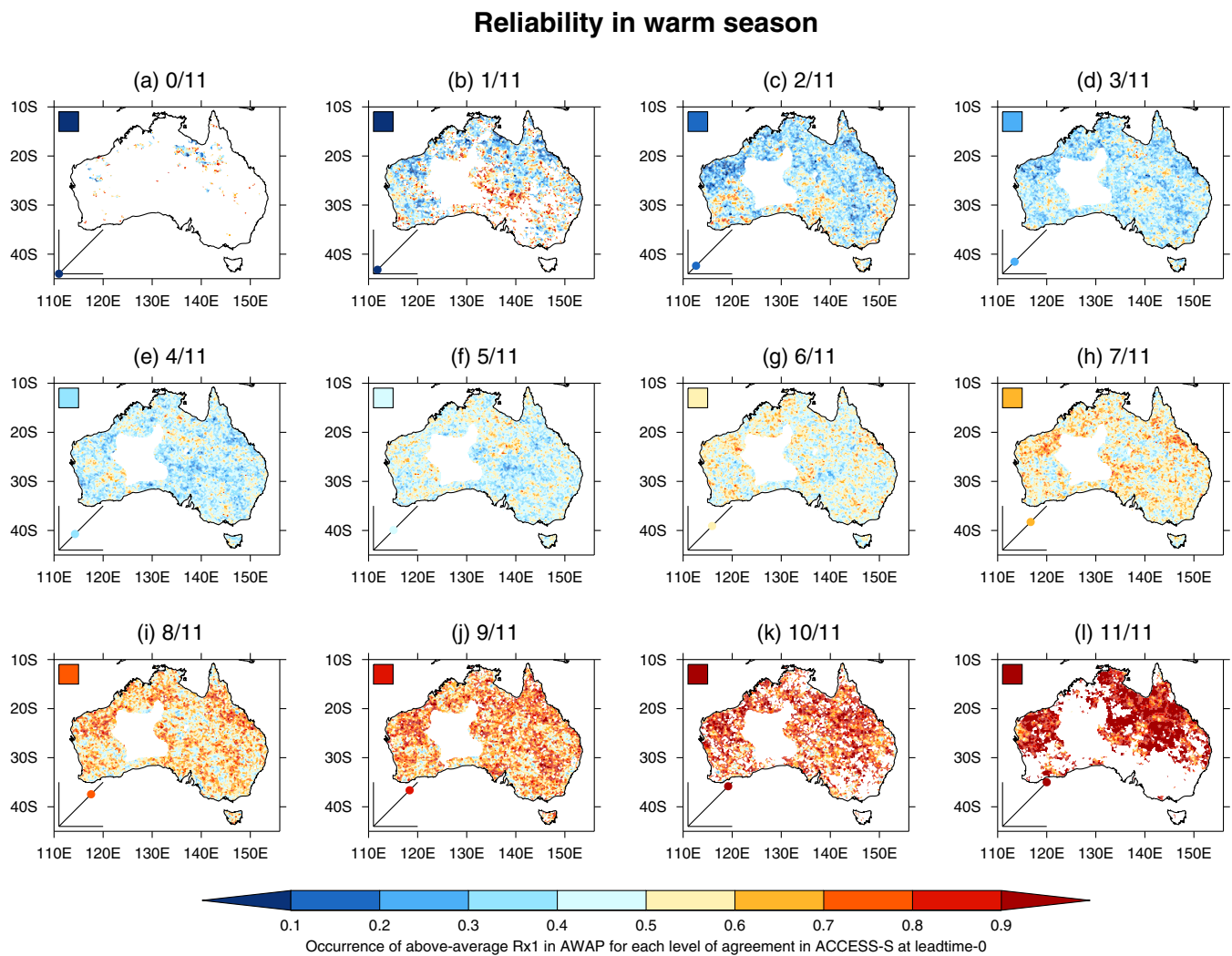


FIGURE 7 (a–l) Maps representing the reliability in Rx1day lead-0 predictions in the warm season (November–April). For cases when each possible fraction of the ACCESS-S1 ensemble is above average, the fraction of corresponding observed values that are above average is shown. The fraction is only shown where there are at least five occurrences where ACCESS-S1 has the fraction of above-average ensemble members considered. The expected colour if ACCESS-S1 is performing well is shown in the top left of each plot and a graphical representation of the point on a reliability diagram being investigated is shown in the bottom-left of each plot [Colour figure can be viewed at wileyonlinelibrary.com]

forecast wetter-than-normal conditions across the rainfall indices for much of Australia even at one-to-two-month lead-times. Given that December is the calendar month in which ACCESS-S1 appears to have the worst performance based on the previous results (e.g. Figure 2), it is also promising that for a particularly extreme event as occurred in December 2010, there is some evidence of ACCESS-S1 providing useful forecasts in unusually extreme circumstances.

The other case-study examined was June 2007 when an East Coast Low brought extreme rainfall to coastal New South Wales (Mills *et al.*, 2010). While the north and east of Australia were unusually wet, most of the south including Tasmania was drier than normal (Figure 12) as high-pressure systems were located over the Great

Australian Bight for much of the month. The lead-0 forecasts (from 1 June 2007) performed well in capturing the pattern of very wet anomalies in the east and the dry conditions in the south. At longer lead-times (simulations initialised on 1 April 2007 and 1 May 2007) the ACCESS-S1 forecasts performed considerably less well in capturing the extreme wet anomalies in the east, although the drier anomalies in the south are better predicted.

7 | DISCUSSION AND CONCLUSIONS

In this study we have sought to assess forecast performance in seasonal outlooks of precipitation extremes in Australia

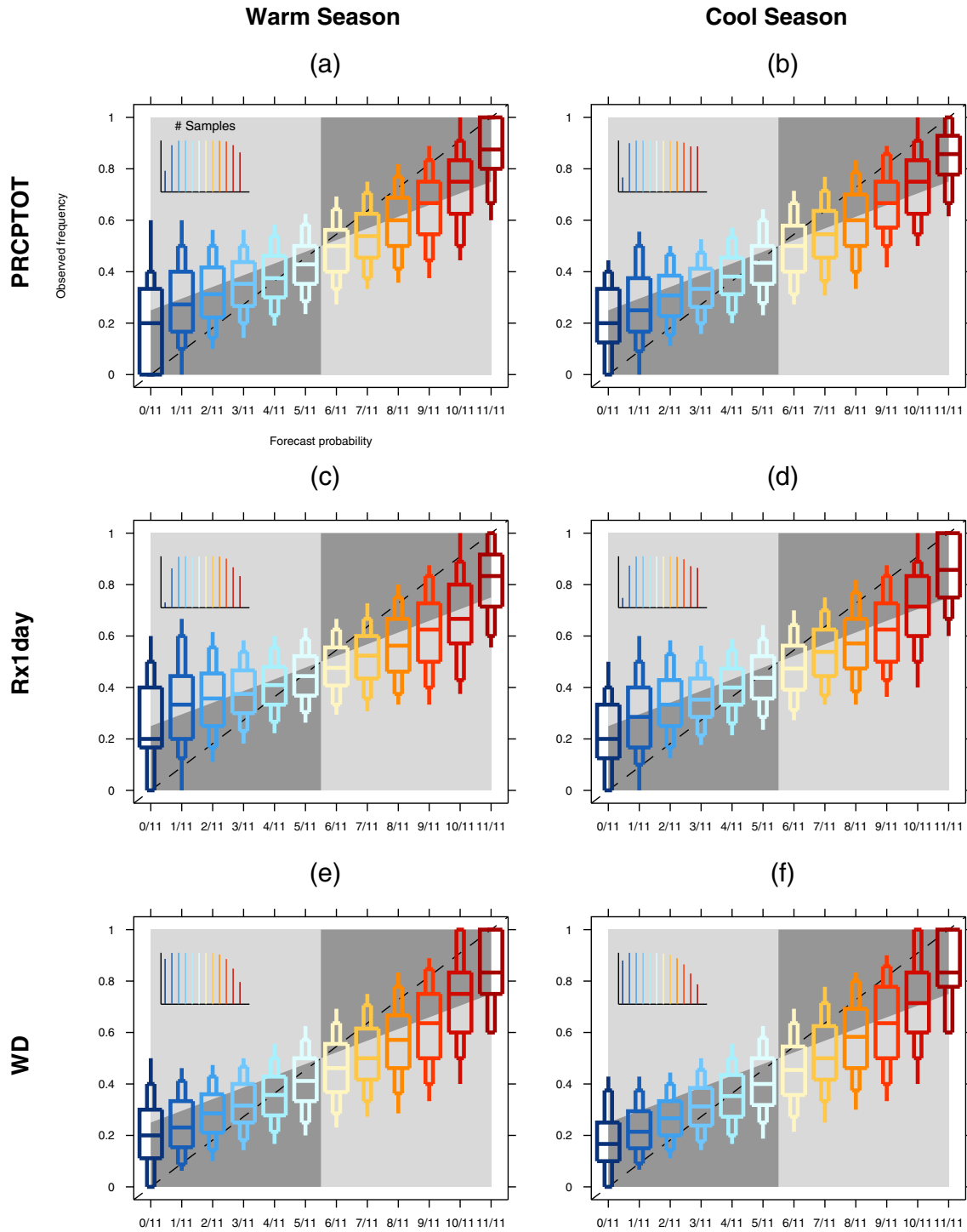


FIGURE 8 Reliability diagrams aggregating locations across Australia. For each forecast probability of above-average conditions in (a,b) PRCPTOT, (c,d) Rx1day, and (e,f) WD in the warm and cool season respectively, the corresponding observed occurrence is shown with the box-plot representing the range of occurrences across Australia. The box plots use the same percentiles as those in Figure 6. The colours are chosen to match those in Figure 7. Miniature graphs in the top-left of each plot indicate the number of locations contributing to each box-plot as a proportion of the maximum number. The dark grey area shows where a positive contribution to Brier skill score is made. The 1:1 line is shown as a dashed black line [Colour figure can be viewed at wileyonlinelibrary.com]

using ACCESS-S1, the current BoM seasonal prediction system. We firstly illustrated that there is a strong potential for predicting some rainfall extremes indices due to the

strong teleconnections that exist with climate modes, such as ENSO. Using a range of different measures, we have found that ACCESS-S1 exhibits a similar degree of model

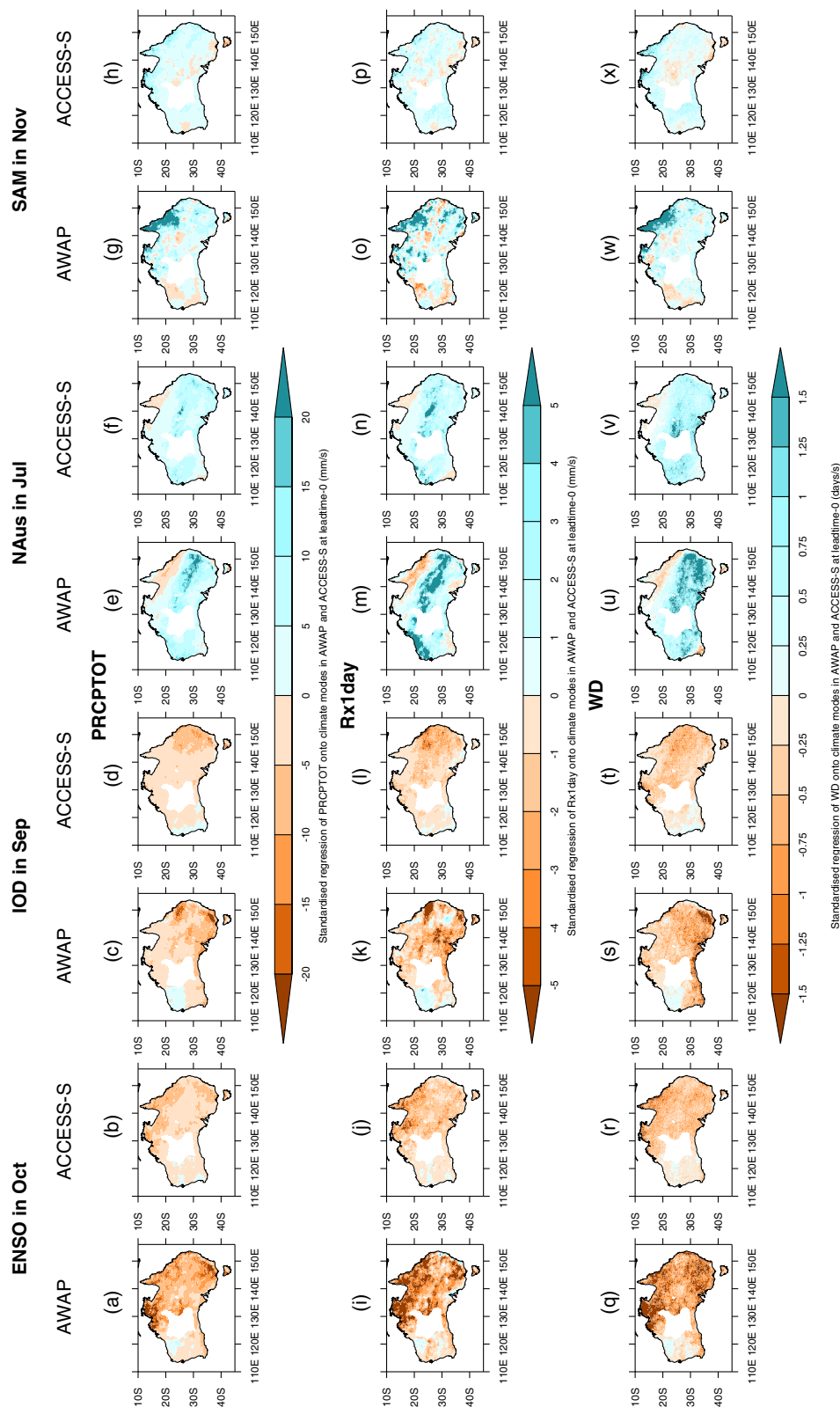


FIGURE 9 Standardised regression coefficients of mean and extreme rainfall indices onto each climate mode index in the 1990–2012 period for selected months with strong mean and extreme rainfall relationships to these modes in AWAP and the ACCESS-SI ensemble median respectively. Regression coefficients are shown for (a–h) PRCPTOT, (i–p) Rx1day, and (q–x) WD [Colour figure can be viewed at wileyonlinelibrary.com]

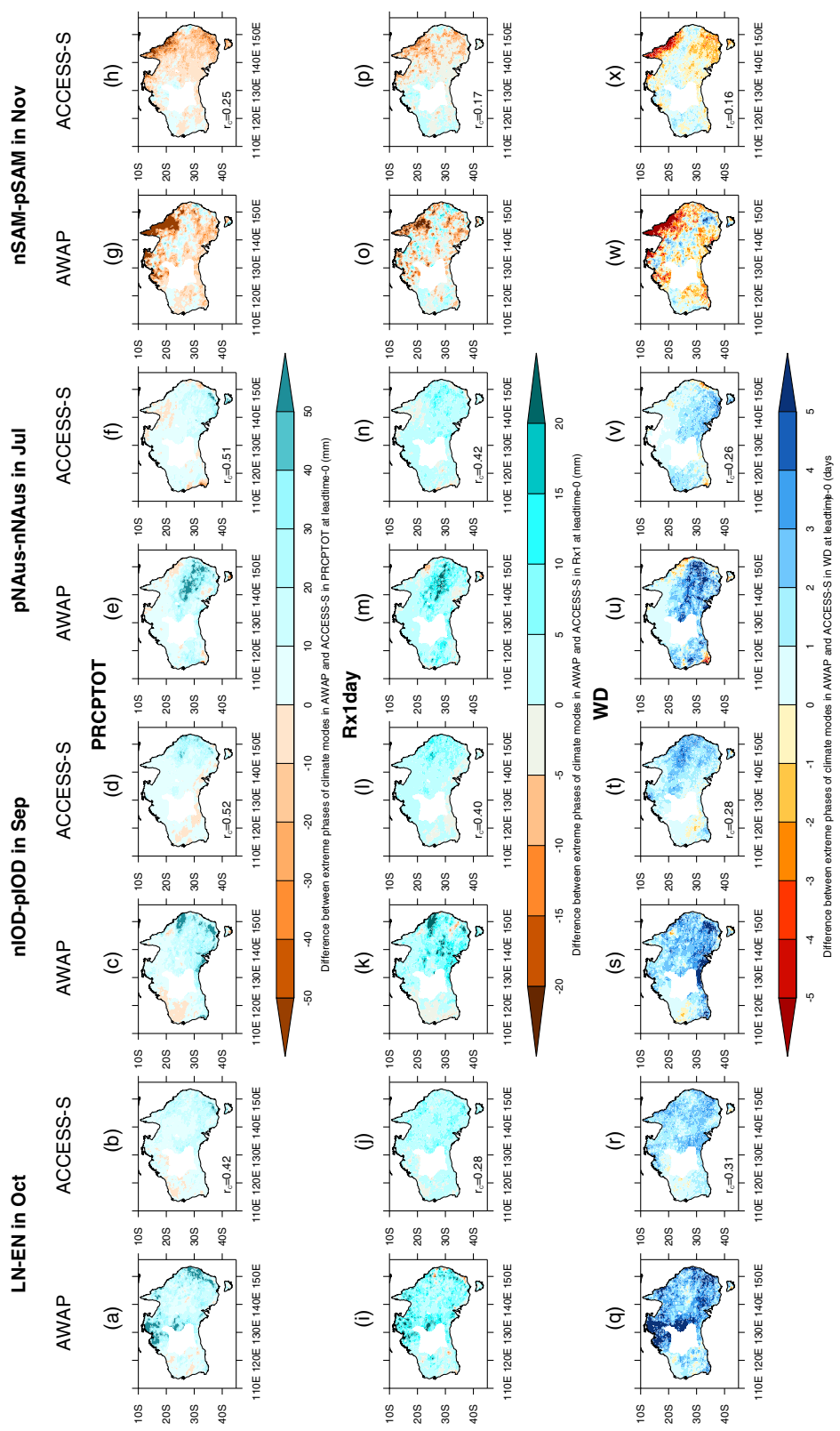


FIGURE 10 Composite median differences for the five most extreme positive and negative values of each climate mode index observed in the 1990–2012 period (months selected shown in Table 2) for months with strong mean and extreme rainfall relationships to these modes in AWAP and the ACCESS-S1 ensemble median respectively. Differences are shown for (a–h) PRCPTOT, (i–p) Rx1day, and (q–x) WD. The Spearman rank pattern correlation between the corresponding ACCESS-S1 and AWAP difference maps is shown in each ACCESS-S1 plot [Colour figure can be viewed at wileyonlinelibrary.com].

performance in the WD index as it does for mean precipitation. ACCESS-S1 is less skilful in predictions of extreme rainfall indices, particularly in more “extreme” extreme indices that represent rarer extremes, such as total rainfall on days above the 90th percentile. ACCESS-S1 performs reasonably well in capturing teleconnections between climate modes and rainfall indices, and in the predictability of rainfall indices during strong phases of climate modes. In our December 2010 case-study, ACCESS-S1 performed well at lead-1 month.

Further analysis of ACCESS-S1 to understand model biases, ensemble overconfidence, and poor model performance in some indices is required, especially in late spring and early summer when the wet season often begins and seasonal outlooks for rainfall are especially useful. Indeed, while not a surprising result, it is disappointing that the model performs relatively poorly in populated areas of the continent where extreme rainfall can have more economically costly impacts, so research that would lead to improved performance in future iterations of ACCESS-S around Sydney, Melbourne and other major cities would be of particular use.

Indices where ACCESS-S1 performs poorly tend to be those which are more spatially inhomogeneous and less strongly associated with variations in mean precipitation (Figure S9). In December, when ACCESS-S1 performance is particularly poor, there are relatively weak observed relationships between climate modes and Australian mean and extreme rainfall indices (Figure 1d), so it may be that without strong teleconnections, rainfall anomalies are driven by mesoscale-to-synoptic-scale processes that are more randomly driven than otherwise is the case, and thus more difficult to forecast on seasonal time-scales.

The analysis of subseasonal-to-seasonal prediction in daily-scale climate extremes is an emerging field (Sillmann *et al.*, 2017) with few analyses to date (Pepler *et al.*, 2015a; Lee *et al.*, 2017) and some focussed solely on temperature extremes (Hudson and Marshall, 2016; Bhend *et al.*, 2017). This is the first comprehensive analysis of sub-seasonal to seasonal prediction of daily-scale rainfall extremes in Australia. As this field is relatively new, and seasonal prediction models continue to improve such that forecasting of extremes becomes more viable, the issue of suitable model performance verification for extreme indices will become more pressing. Here, we used modified versions of common verification measures to assess performance in the ACCESS-S1 model. For instance, we constructed climatologies of median-values instead of means and produced maps of correlation coefficients between ACCESS-S1 and our observational dataset using the non-parametric Spearman rank method instead of Pearson correlations. For some extreme indices there are performance metrics that are less useful than others. In particular, proportion

correct, when applied to the sign of anomalies, is of little use for indices where the median is zero. It could also be misinterpreted for indices like the number of wet days if the climatology is a median, as there is the potential for a high proportion of predicted and observed values to be exactly average rather than above or below average. The use of a combination of metrics and careful application after some modifications was necessary. For more “extreme” indices than were considered here, which tend to be the indices that would signify rarer high-impact events, the issue of suitable model performance verification becomes even more important and sample size limitations become more of an issue. More extreme rainfall indices tend to be more spatially inhomogeneous (e.g. King *et al.*, 2014), so location-specific measures of model performance that perform well in mean rainfall may be of less use as the spatial pattern of an index becomes noisier. Performance measures that draw on techniques used for verification of highly localised extreme rainfall events in high-resolution numerical weather prediction models (e.g. Ebert and McBride, 2000; Roberts, 2008) may be of use for more “extreme” extreme indices that represent only rarer events than those captured by the indices examined here.

The indices for extreme rainfall used here were based on the ETCCDI extreme rainfall indices (Zhang *et al.*, 2011), more commonly used for climate change detection and modelling (e.g. Donat *et al.*, 2013; Sillmann *et al.*, 2013). The analysis of ACCESS-S1 performance in these indices is useful in understanding model biases and other issues, but we have not determined the utility of these indices for seasonal prediction in conjunction with relevant stakeholder groups. Previous work has indicated that for seasonal prediction to be of greatest use to stakeholders, the predictive skill is only one factor amongst several that determine whether seasonal outlooks will be used in decision-making processes (Hartmann *et al.*, 2002; Zier-vogel and Downing, 2004). Given the demonstrable performance in predicting some rainfall indices in ACCESS-S1, further work to determine which indices would be of use to specific stakeholder groups and how they will inform decisions is required.

The analysis we have conducted is primarily focussed on forecasts for the month ahead, but our analysis for longer lead-times suggests a substantial decrease in model performance. There may be more promising results if extremes indices are designed for the analysis of sub-seasonal prediction (Hudson *et al.*, 2011; Marshall *et al.*, 2014), such as on time-scales of two-to-three or three-to-four weeks. For shorter time-windows the extremes indices would need to be redesigned to be relevant on the time-scale of a week rather than a month.

It is likely that some of the model performance in the lead-0 forecasts is due to predictability on the time-scale of

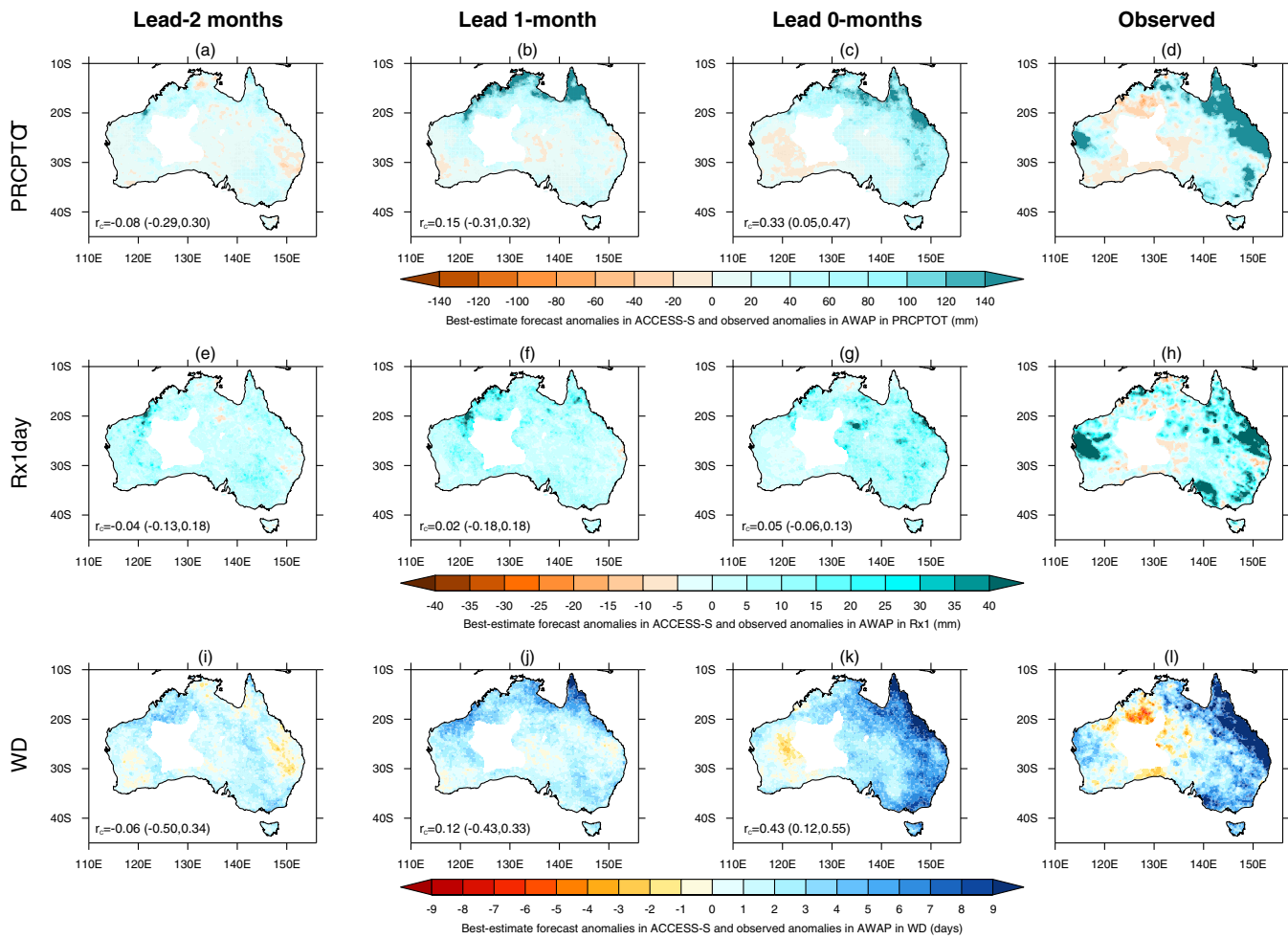


FIGURE 11 For the extreme wet month of December 2010, the ACCESS-S1 ensemble median anomalies at lead-2, lead-1, and lead-0 are shown with the observed anomalies in (a–d) PRCPTOT, (e–h) Rx1day, and (i–l) WD. Stippling shows at least three-quarters of ensemble members are of the same sign. The median Spearman rank pattern correlation coefficients between the ACCESS-S1 and observed anomalies are shown in the bottom-left of each plot with the lowest and highest pattern correlation coefficients across the ACCESS-S1 ensemble in parentheses [Colour figure can be viewed at wileyonlinelibrary.com]

numerical weather prediction, and this is suggested from the reduced performance in ACCESS-S1 for simulations initialised several days before the start of the month compared with 1st of the month simulations (Figure 5). If an extreme rainfall event is forecast to occur in the first 7 to 10 days after the runs are initialised, there is more likely to be more consistency across the ensemble in the anomalies associated with extreme rainfall indices. This effect may be part of the reason that the June 2007 prediction (Figure 12), initialised on 1 June, was particularly accurate as the East Coast Low (ECL) brought the heaviest rainfall on 7 June. In contrast, in December 2010 (Figure 11), where the lead-0 forecasts still perform well, the heaviest rainfall occurred near the end of the month in most of the northeast of Australia. More generally, the model performance of seasonal predictions of rainfall extremes is likely to be connected to the predictability of the weather systems that bring the extreme rainfall

and this will vary greatly. For instance, ECLs, in common with other mesoscale systems over Australia, are not strongly related to climate modes (Pepler *et al.*, 2015b) and require the confluence of several important ingredients to occur (Cavicchia *et al.*, 2019). It is likely that ECLs have less inherent predictability than other major rain-bearing systems including tropical cyclones which have stronger relationships to climate modes such as ENSO (Kuleshov *et al.*, 2008; Dowdy *et al.*, 2012). This effect likely contributes to the pattern of model performance across Australia with greater model fidelity in northern areas and the interior than in the south and near coasts.

The results of this analysis are drawn from a 23-year hindcast set of ACCESS-S1 simulations, and focussed on first-of-the-month simulations to ensure consistency, for the 1990–2012 period. This is below the 30 years that the World Meteorological Organisation would use to define

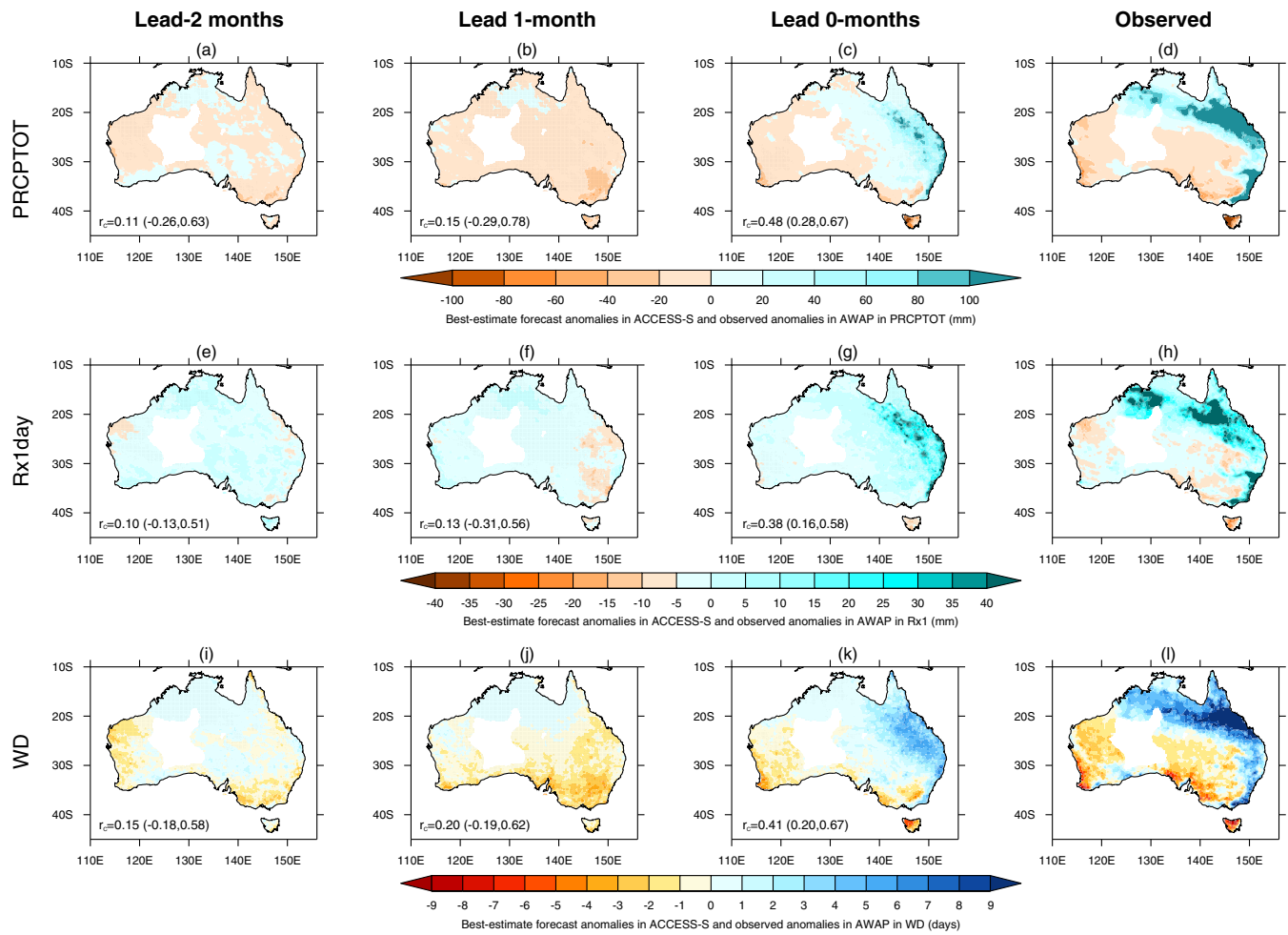


FIGURE 12 (a–l) As Figure 11 but for June 2007 [Colour figure can be viewed at wileyonlinelibrary.com]

climatologies. Thus, there is an assumption that this period and length of period are sufficient in assessing the performance of ACCESS-S1. A period of 23 years is typically too short to obtain statistically robust results, particularly for aspects of the prediction system that are inherently noisy, such as relatively localised forecasts. In addition, a sufficiently long hindcast set is necessary for including an adequate number of cases of the low-frequency influences on Australian climate, like the different phases of ENSO, and for knowing how model performance may vary based on the state of these climate drivers. Furthermore, teleconnections between climate modes and specific weather systems have been shown to be variable in the past with consequences for skill in statistical seasonal forecasts, such as has been the case with the ENSO–Indian Monsoon relationship (Kumar *et al.*, 1999). Teleconnections between ENSO and Australian climate have some decadal-scale variability related to the Interdecadal Pacific Oscillation (Power *et al.*, 2006; Cai and van Renssch, 2012; King *et al.*, 2013a; Lim *et al.*, 2017) so there is the possibility that the 23-year hindcast period does not optimally represent the recent Australian climate and its variability.

For the next version of ACCESS-S (version 2), there will be a longer hindcast period of at least 30 years. While it is promising that the teleconnections between climate modes and mean and extreme rainfall indices are broadly captured in the 23-year ACCESS-S1 hindcast, further analysis of teleconnections using a longer hindcast would be useful.

Overall, in this analysis we have found that sub-seasonal prediction of some rainfall indices in Australia may be viable using the BoM operational model, ACCESS-S1, but that performance decreases rapidly beyond the first forecast month. A substantial component of forecast performance at lead-0 is due to skill on the timeframe of weather prediction, so seasonal prediction is unlikely to be possible but sub-seasonal outlooks, extending beyond the current forecasts of likelihood of above- or below-average total rainfall, may be useful. Forecasts based on indices such as the probability of above- or below-average number of wet days and intensity of the wettest day are possible. Further work will be needed to determine the usefulness of such indices in sub-seasonal outlooks.

ACKNOWLEDGEMENTS

We thank the editor for handling our manuscript and we thank Nicholas Klingaman and an anonymous reviewer for their constructive feedback on our article. Andrew King and Todd Lane were funded by the Australian Research Council (DE180100638 and CE170100023 respectively). Debra Hudson, Eun-Pa Lim, Andrew Marshall and Harry Hendon's contribution is part of the Forewarned is Forearmed project, which is supported by funding from the Australian Government Department of Agriculture as part of its Rural Research and Development for Profit programme. The work was undertaken with the assistance of resources from the National Computational Infrastructure (NCI), which is supported by the Australian Government.

ORCID

Andrew D. King  <https://orcid.org/0000-0001-9006-5745>

Debra Hudson  <https://orcid.org/0000-0002-0129-0922>

Todd P. Lane  <https://orcid.org/0000-0003-0171-6927>

REFERENCES

- Alves, O., Wang, G., Zhong, A., Smith, N., Tseitkin, F., Warren, G., Schiller, A., Godfrey, S. and Meyers, G. (2003). *POAMA: Bureau of Meteorology operational coupled model seasonal forecast system*. Brisbane: National Drought Forum Report, pp. 49–56.
- Australian Business Roundtable for Disaster Resilience and Safer Communities 2016 *The economic cost of the social impact of natural disasters* (Sydney). Available at: <http://australianbusinessroundtable.com.au/assets/documents/Report%20-%20Social%20costs/Report%20-%20The%20economic%20cost%20of%20the%20social%20impact%20of%20natural%20disasters.pdf> [Accessed 23 December 2019].
- Bhend, J., Mahlstein, I. and Liniger, M.A. (2017). Predictive skill of climate indices compared to mean quantities in seasonal forecasts. *Quarterly Journal of the Royal Meteorological Society*, 143(702), 184–194. [http://doi.wiley.com/10.1002/qj.2908](https://doi.wiley.com/10.1002/qj.2908).
- Bureau of Meteorology 2019 *Operational implementation of ACCESS-S1 forecast post-processing* (Melbourne) Available at: <http://www.bom.gov.au/australia/charts/bulletins/opsull-124-ext.pdf> [Accessed 03 February 2020].
- de Burgh-Day, C.O., Spillman, C.M., Stevens, C., Alves, O. and Rickard, G. (2019). Predicting seasonal ocean variability around New Zealand using a coupled ocean–atmosphere model. *New Zealand Journal of Marine and Freshwater Research*, 53, 201–221 <https://www.tandfonline.com/doi/full/10.1080/00288330.2018.1538052>.
- Cai, W. and van Renssch, P. (2012). The 2011 southeast Queensland extreme summer rainfall: a confirmation of a negative Pacific Decadal Oscillation phase? *Geophysical Research Letters*, 39(8), L08702 [http://doi.wiley.com/10.1029/2011GL050820](https://doi.wiley.com/10.1029/2011GL050820).
- Camp, J., Wheeler, M.C., Hendon, H.H., Gregory, P.A., Marshall, A.G., Tory, K.J., Watkins, A.B., MacLachlan, C. and Kuleshov, Y. (2018). Skilful multiweek tropical cyclone prediction in ACCESS-S1 and the role of the MJO. *Quarterly Journal of the Royal Meteorological Society*, 144(714), 1337–1351 [http://doi.wiley.com/10.1002/qj.3260](https://doi.wiley.com/10.1002/qj.3260).
- Catto, J.L., Nicholls, N. and Jakob, C. (2012). North Australian sea surface temperatures and the El Niño–Southern Oscillation in observations and models. *Journal of Climate*, 25, 5011–5029 <http://journals.ametsoc.org/doi/abs/10.1175/JCLI-D-11-00311.1>.
- Cavicchia, L., Pepler, A., Dowdy, A. and Walsh, K. (2019). A physically based climatology of the occurrence and intensification of Australian East Coast Lows. *Journal of Climate*, 32, 2823–2841. <http://journals.ametsoc.org/doi/10.1175/JCLI-D-18-0549.1>.
- Cottrill, A., Hendon, H.H., Lim, E.-P., Langford, S., Shelton, K., Charles, A., McClymont, D., Jones, D. and Kuleshov, Y. (2013). Seasonal forecasting in the Pacific using the coupled model POAMA-2. *Weather and Forecasting*, 28, 668–680 <http://journals.ametsoc.org/doi/abs/10.1175/WAF-D-12-00072.1>.
- Donat, M.G., Alexander, L.V., Yang, H., Durre, I., Vose, R., Dunn, R.J.H., Willett, K.M., Aguilar, E., Brunet, M., Caesar, J., Hewittson, B., Jack, C., Klein Tank, A.M.G., Kruger, A.C., Marengo, J., Peterson, T.C., Renom, M., Oria Rojas, C., Rusticucci, M., Salinger, J., Elrayah, A.S., Sekele, S.S., Srivastava, A.K., Trewin, B., Villarroel, C., Vincent, L.A., Zhai, P., Zhang, X. and Kitching, S. (2013). Updated analyses of temperature and precipitation extreme indices since the beginning of the twentieth century: the HadEX2 dataset. *Journal of Geophysical Research: Atmospheres*, 118, 2098–2118 <http://doi.wiley.com/10.1002/jgrd.50150>.
- Dowdy, A.J., Qi, L., Jones, D., Ramsay, H., Fawcett, R. and Kuleshov, Y. (2012). Tropical cyclone climatology of the South Pacific Ocean and its relationship to El Niño–Southern Oscillation. *Journal of Climate*, 25, 6108–6122 <http://journals.ametsoc.org/doi/abs/10.1175/JCLI-D-11-00647.1>.
- Drosdowsky, W. and Chambers, L.E. (2000). Near-global sea surface temperature anomalies as predictors of Australian seasonal rainfall. *Journal of Climate*, 14, 1677–1687 <https://journals.ametsoc.org/doi/pdf/10.1175/1520-0442%282001%29014%3C1677%3ANACNGS%3E2.0.CO%3B2>.
- Ebert, E. and McBride, J. (2000). Verification of precipitation in weather systems: determination of systematic errors. *Journal of Hydrology*, 239, 179–202 <https://www.sciencedirect.com/science/article/pii/S0022169400003437>.
- Evans, J.P. and Boyer-Souchet, I. (2012). Local sea surface temperatures add to extreme precipitation in northeast Australia during La Niña. *Geophysical Research Letters*, 39(10) L10803 <http://doi.wiley.com/10.1029/2012GL052014>.
- Hartmann, H.C., Pagano, T.C., Sorooshian, S. and Bales, R. (2002). Confidence builders: evaluating seasonal climate forecasts from user perspectives. *Bulletin of the American Meteorological Society*, 83, 683–698 <http://journals.ametsoc.org/doi/abs/10.1175/1520-0477%282002%29083%3C0683%3ACBESCF%3E2.3.CO%3B2>.
- Haylock, M. and Nicholls, N. (2000). Trends in extreme rainfall indices for an updated high quality data set for Australia, 1910–1998. *International Journal of Climatology*, 20, 1533–1541 <http://doi.wiley.com/10.1002/1097-0088%2820001115%2920%3A13%3C1533%3A%3AAID-JOC586%3E3.0.CO%3B2-J>.
- Hendon, H.H., Lim, E.-P. and Nguyen, H. (2014). Seasonal variations of subtropical precipitation associated with the southern annular mode. *Journal of Climate*, 27, 3446–3460 <http://journals.ametsoc.org/doi/abs/10.1175/JCLI-D-13-00550.1>.
- van den Honert, R.C. and McAneney, J. (2011). The 2011 Brisbane floods: causes, impacts and implications. *Water*, 3, 1149–1173 <http://www.mdpi.com/2073-4441/3/4/1149>.

- Hudson, D., Alves, O., Hendon, H.H., Lim, E.-P., Liu, G., Luo, J.-J., MacLachlan, C., Marshall, A.G., Shi, L., Wang, G., Wedd, R., Young, G., Zhao, M. and Zhou, X. (2017). ACCESS-S1: the new Bureau of Meteorology multi-week to seasonal prediction system. *Journal of Southern Hemisphere Earth Systems Science*, 67(3), 132–159 <http://www.bom.gov.au/jshess/docs/2017/Hudson.pdf>.
- Hudson, D., Alves, O., Hendon, H.H. and Marshall, A.G. (2011). Bridging the gap between weather and seasonal forecasting: intraseasonal forecasting for Australia. *Quarterly Journal of the Royal Meteorological Society*, 137, 673–689 <http://doi.wiley.com/10.1002/qj.769>.
- Hudson D and Marshall A G. 2016 *Extending the Bureau's heatwave forecast to multi-week timescales (Melbourne)*. Available at: <http://www.bom.gov.au/research/publications/researchreports/BRR-016.pdf> [Accessed 15 July 2019].
- Jones, D.A., Wang, W. and Fawcett, R. (2009). High-quality spatial climate data-sets for Australia. *Australian Meteorological and Oceanographic Journal*, 58, 233–248 http://www.bom.gov.au/jshess/docs/2009/jones_hres.pdf.
- King, A.D., Alexander, L.V. and Donat, M.G. (2013a). Asymmetry in the response of eastern Australia extreme rainfall to low-frequency Pacific variability. *Geophysical Research Letters*, 40(10), 2271–2277.
- King, A.D., Alexander, L.V. and Donat, M.G. (2013b). The efficacy of using gridded data to examine extreme rainfall characteristics: a case study for Australia. *International Journal of Climatology*, 33(10), 2376–2387.
- King, A.D., Klingaman, N.P., Alexander, L.V., Donat, M.G., Jourdain, N.C. and Maher, P. (2014). Extreme rainfall variability in Australia: patterns, drivers, and predictability. *Journal of Climate*, 27, 6035–6050 <http://journals.ametsoc.org/doi/abs/10.1175/JCLI-D-13-00715.1>.
- Klingaman, N.P., Woolnough, S.J. and Syktus, J. (2013). On the drivers of inter-annual and decadal rainfall variability in Queensland, Australia. *International Journal of Climatology*, 33, 2413–2430 <http://doi.wiley.com/10.1002/joc.3593>.
- Kuleshov, Y., Qi, L., Fawcett, R. and Jones, D. (2008). On tropical cyclone activity in the Southern Hemisphere: trends and the ENSO connection. *Geophysical Research Letters*, 35, L14S08 <http://doi.wiley.com/10.1029/2007GL032983>.
- Kumar, K.K., Rajagopalan, B. and Cane, M.A. (1999). On the weakening relationship between the Indian monsoon and ENSO. *Science*, 284, 2156–2159 <http://www.ncbi.nlm.nih.gov/pubmed/10381876>.
- Lee, S.-S., Moon, J.-Y., Wang, B. and Kim, H.-J. (2017). Subseasonal prediction of extreme precipitation over Asia: boreal summer intraseasonal oscillation perspective. *Journal of Climate*, 30, 2849–2865 <http://journals.ametsoc.org/doi/10.1175/JCLI-D-16-0206.1>.
- Lim, E.-P. and Hendon, H.H. (2015). Understanding and predicting the strong southern annular mode and its impact on the record wet east Australian spring 2010. *Climate Dynamics*, 44, 2807–2824 <http://link.springer.com/10.1007/s00382-014-2400-5>.
- Lim, E.-P., Hendon, H.H., Zhao, M. and Yin, Y. (2017). Inter-decadal variations in the linkages between ENSO, the IOD and south-eastern Australian springtime rainfall in the past 30 years. *Climate Dynamics*, 49, 97–112 <http://link.springer.com/10.1007/s00382-016-3328-8>.
- MacLachlan, C., Arribas, A., Peterson, K.A., Maidens, A., Fereday, D., Scaife, A.A., Gordon, M., Vellinga, M., Williams, A., Comer, R.E., Camp, J., Xavier, P. and Madec, G. (2015). Global seasonal forecast system version 5 (GloSea5): a high-resolution seasonal forecast system. *Quarterly Journal of the Royal Meteorological Society*, 141, 1072–1084 <http://doi.wiley.com/10.1002/qj.2396>.
- Marshall, A.G. and Hendon, H.H. (2019). Multi-week prediction of the Madden-Julian Oscillation with ACCESS-S1. *Climate Dynamics*, 52, 2513–2528 <http://link.springer.com/10.1007/s00382-018-4272-6>.
- Marshall, A.G., Hudson, D., Wheeler, M.C., Alves, O., Hendon, H.H., Pook, M.J. and Risbey, J.S. (2014). Intra-seasonal drivers of extreme heat over Australia in observations and POAMA-2. *Climate Dynamics*, 43, 1915–1937 <http://link.springer.com/10.1007/s00382-013-2016-1>.
- McBride, J.L. and Nicholls, N. (1983). Seasonal relationships between Australian rainfall and the Southern Oscillation. *Monthly Weather Review*, 111, 1998–2004 <http://journals.ametsoc.org/doi/abs/10.1175/1520-0493%281983%29111%3C1998%3ASRBARA%3E2.0.CO%3B2>.
- Mills G A, Webb R, Davidson N E, Kepert J, Seed A and Abbs D. 2010 *The Pasha Bulker east coast low of 8 June 2007*. Available at: https://www.researchgate.net/profile/Jeffrey_Kepert/publication/277295660_Subjects_Meteorology-Research_Climatic_changes-Research/links/55c0204708ae092e9666a6db.pdf [Accessed 21 May 2019].
- Min, S.-K., Cai, W. and Whetton, P. (2013). Influence of climate variability on seasonal extremes over Australia. *Journal of Geophysical Research*, 118, 643–654 <http://doi.wiley.com/10.1002/jgrd.50164>.
- Nicholls, N. (1979). A possible method for predicting seasonal tropical cyclone activity in the Australian region. *Monthly Weather Review*, 107, 1221–1224 <http://journals.ametsoc.org/doi/abs/10.1175/1520-0493%281979%29107%3C1221%3AAPMFPS%3E2.0.CO%3B2>.
- Nicholls, N. (1983). The potential for long-range prediction of seasonal mean temperature in Australia. *Australian Meteorological Magazine*, 31, 203–207.
- Nicholls, N. (1984). The Southern Oscillation, sea-surface-temperature, and interannual fluctuations in Australian tropical cyclone activity. *International Journal of Climatology*, 4, 661–670 <http://doi.wiley.com/10.1002/joc.3370040609>.
- Nicholls, N. (1985). Predictability of interannual variations of Australian seasonal tropical cyclone activity. *Monthly Weather Review*, 113, 1144–1149 <http://journals.ametsoc.org/doi/abs/10.1175/1520-0493%281985%29113%3C1144%3APOIVOA%3E2.0.CO%3B2>.
- Nicholls, N., Drosdowsky, W. and Lavery, B. (1997). Australian rainfall variability and change. *Weather*, 52(3), 66–72 <http://doi.wiley.com/10.1002/j.1477-8696.1997.tb06274.x>.
- Nicholls, N. and Woodcock, F. (1981). Verification of an empirical long-range weather forecasting technique. *Quarterly Journal of the Royal Meteorological Society*, 107, 973–976 <http://doi.wiley.com/10.1002/qj.49710745415>.
- Pepler, A.S., Díaz, L.B., Prodhomme, C. and Doblas-Reyes, F.J. (2015a). The ability of a multi-model seasonal forecasting ensemble to forecast the frequency of warm, cold and wet extremes. *Search Results*, 9, 68–77 <https://www.sciencedirect.com/science/article/pii/S2212094715300062>.

- Pepler, A.S., Di Luca, A., Ji, F., Alexander, L.V., Evans, J.P. and Sherwood, S.C. (2015b). Impact of identification method on the inferred characteristics and variability of Australian East Coast Lows. *Monthly Weather Review*, 143, 864–877 <http://journals.ametsoc.org/doi/10.1175/MWR-D-14-00188.1>.
- Power, S., Haylock, M., Colman, R. and Wang, X. (2006). The predictability of interdecadal changes in ENSO activity and ENSO teleconnections. *Journal of Climate*, 19, 4755–4771 <http://journals.ametsoc.org/doi/abs/10.1175/JCLI3868.1>.
- Quayle, E.T. (1929). Long range rainfall forecasting from tropical (Darwin) air pressures. *Proceedings of the Royal Society of Victoria*, 41, 160–164.
- Rayner, N.A., Parker, D.E., Horton, E.B., Folland, C.K., Alexander, L.V., Rowell, D.P., Kent, E.C. and Kaplan, A. (2003). Global analyses of sea surface temperature, sea ice, and night marine air temperature since the late nineteenth century. *Journal of Geophysical Research*, 108(D14), 4407 <http://doi.wiley.com/10.1029/2002JD002670>.
- Risbey, J.S., Pook, M.J., McIntosh, P.C., Wheeler, M.C. and Hendon, H.H. (2009). On the remote drivers of rainfall variability in Australia. *Monthly Weather Review*, 137, 3233–3253 <http://journals.ametsoc.org/doi/abs/10.1175/2009MWR2861.1>.
- Roberts, N. (2008). Assessing the spatial and temporal variation in the skill of precipitation forecasts from an NWP model. *Meteorological Applications*, 15, 163–169 <http://doi.wiley.com/10.1002/met.57>.
- Saji, N.H., Goswami, B.N., Vinayachandran, P.N. and Yamagata, T. (1999). A dipole mode in the tropical Indian Ocean. *Nature*, 401, 360–363 <http://www.nature.com/articles/43854>.
- Sillmann, J., Kharin, V.V., Zhang, X., Zwiers, F.W. and Branaugh, D. (2013). Climate extremes indices in the CMIP5 multimodel ensemble. Part 1: Model evaluation in the present climate. *Journal of Geophysical Research: Atmospheres*, 118, 1716–1733 <http://doi.wiley.com/10.1002/jgrd.50203>.
- Sillmann, J., Thorarinsdottir, T., Keenlyside, N., Schaller, N., Alexander, L.V., Hegerl, G., Seneviratne, S.I., Vautard, R., Zhang, X. and Zwiers, F.W. (2017). Understanding, modeling and predicting weather and climate extremes: challenges and opportunities. *Weather and Climate Extremes*, 18, 65–74 <https://www.sciencedirect.com/science/article/pii/S2212094717300440#bib102>.
- Smith, G. and Spillman, C. (2019). New high-resolution sea surface temperature forecasts for coral reef management on the Great Barrier Reef. *Coral Reefs*, 38(5), 1039–1056 <http://link.springer.com/10.1007/s00338-019-01829-1>.
- Stone, R.C., Hammer, G.L. and Marcussen, T. (1996). Prediction of global rainfall probabilities using phases of the Southern Oscillation Index. *Nature*, 384, 252–255 <http://www.nature.com/doifinder/10.1038/384252a0>.
- The Centre for International Economics 2014a *Analysis of the benefits of improved seasonal climate forecasting*. Available at: <http://www.managingclimate.gov.au/wp-content/uploads/2014/05/MCV-CIE-report-Value-of-improved-forecasts-non-agriculture-2014.pdf> [Accessed 03 April 2018].
- The Centre for International Economics 2014b *Analysis of the benefits of improved seasonal climate forecasting for agriculture*. Available at: <http://www.managingclimate.gov.au/wp-content/uploads/2014/06/MCV-CIE-report-Value-of-improved-forecasts-agriculture-2014.pdf> [Accessed 03 April 2018].
- Vitart, F., Cunningham, C., DeFlorio, M., Dutra, E., Ferrianti, L., Golding, B., Hudson, D., Jones, C., Lavaysse, C., Robbins, J. and Tippett, M.K. (2019). Sub-seasonal to seasonal prediction of weather extremes. In: Robertson, A. and Vitart, F. (Eds.) *Sub-Seasonal to Seasonal Prediction*. Amsterdam, Netherlands: Elsevier, pp. 365–386 <https://www.sciencedirect.com/science/article/pii/B9780128117149000176>.
- Wilks, D.S. (2010). Sampling distributions of the Brier score and Brier skill score under serial dependence. *Quarterly Journal of the Royal Meteorological Society*, 136, 2109–2118 <http://doi.wiley.com/10.1002/qj.709>.
- Wilks, D.S. (2011). *Statistical Methods in the Atmospheric Sciences*. London, United Kingdom: Elsevier/Academic Press.
- Zhang, X., Alexander, L., Hegerl, G.C., Jones, P., Tank, A.K., Peterson, T.C., Trewin, B. and Zwiers, F.W. (2011). Indices for monitoring changes in extremes based on daily temperature and precipitation data. *Wiley Interdisciplinary Reviews: Climate Change*, 2, 851–870 <http://doi.wiley.com/10.1002/wcc.147>.
- Zervogel, G. and Downing, T.E. (2004). Stakeholder networks: improving seasonal climate forecasts. *Climate Change*, 65, 73–101 <http://link.springer.com/10.1023/B:CLIM.0000037492.18679.9e>.

SUPPORTING INFORMATION

Additional supporting information may be found online in the Supporting Information section at the end of this article.

How to cite this article: King AD, Hudson D, Lim E-P, et al. Sub-seasonal to seasonal prediction of rainfall extremes in Australia. *QJR Meteorol Soc*. 2020;1–22. <https://doi.org/10.1002/qj.3789>